Conformational Transitions of the Sarcoplasmic Reticulum Ca-ATPase Studied by Time-Resolved EPR and Quenched-Flow Kinetics†

James E. Mahaney,‡ Jeffrey P. Froehlich,§ and David D. Thomas*,‡

Department of Biochemistry, University of Minnesota Medical School, Minneapolis, Minnesota 55455, and The National Institute on Aging, National Institutes of Health, Gerontology Research Center, Baltimore City Hospitals, Baltimore, Maryland 21224

Received October 20, 1994; Revised Manuscript Received January 19, 1995⊗

ABSTRACT: We have used time-resolved electron paramagnetic resonance (EPR) and quenched-flow kinetics in order to investigate the dynamics of Ca-ATPase conformational changes involved in Ca^{2+} pumping in sarcoplasmic reticulum (SR) membranes at 2 °C. The Ca-ATPase was selectively labeled with an iodoacetamide spin label (IASL), which yields EPR spectra sensitive to enzyme conformational changes during ATP-induced enzymatic cycling. The addition of ATP, AMPPCP, CrATP, or ADP decreased the rotational mobility of a fraction of the probes, indicating a distinct protein conformational state corresponding to this probe population, while P_i under conditions producing "backdoor" phosphorylation produced no spectral change. Transient changes in the amplitude of the restricted component associated with the pre-steady state of Ca^{2+} pumping were detected with 10 ms time resolution after an [ATP] jump produced by laser flash photolysis of caged ATP in the EPR sample. The laser energy was adjusted to generate 100 μM ATP from 1 mM caged ATP. At 0.1 M KCl, the EPR transient consisted of a brief initial lag phase, a monoexponential phase with a rate of 20 s^{-1}, and a decay back to the initial intensity after the ATP had been consumed. Raising [KCl] from 0.1 to 0.4 M slowed the rate of the exponential phase from 20 to 6 s^{-1}. Lowering the pH from 7 to 6, which increased the rate of caged ATP photolysis, eliminated the lag but did not change the apparent rate of the EPR signal rise. Parallel acid quenched-flow experiments conducted at 0.1 M KCl and 100 μM ATP produced fast (50−58 s^{-1}) and slow (20 s^{-1}) phases of phosphoenzyme formation. Increasing [KCl] from 0.1 to 0.4 M decreased the rate of the slow phase of phosphorylation from 20 to 5 s^{-1}, without affecting the fast phase. The close correlation between the slow phase of phosphorylation and the exponential phase of the EPR signal suggests that the spin probe monitors a conformational event associated with phosphoenzyme formation in a population of catalytic sites with delayed kinetics. We propose that this constraint is imposed by conformational coupling between the catalytic subunits in a Ca-ATPase oligomer and that, consequently, the EPR signal reflects changes in quaternary protein structure as well as changes in secondary and tertiary structure associated with ATP-dependent phosphorylation.

The Ca-ATPase of the sarcoplasmic reticulum (SR)[1] membrane transduces the energy derived from ATP hydrolysis into Ca^{2+} translocation across the membrane through a series of conformational events in the catalytic cycle. A widely accepted model for the Ca-ATPase transport cycle (Scheme 1) involves two fundamental enzyme conformations, E1 and E2, and their phosphorylated counterparts, E1P and E2P, which couple ATP hydrolysis to Ca^{2+} transport through differences in their affinities and specificities for ATP and Ca^{2+}. In the absence of ligands, the resting enzyme exists as a mixture of E1 and E2 states; the presence of micromolar Ca^{2+} shifts the conformational equilibrium (step 8) strongly toward Ca_2·E1 (Froud & Lee, 1985; Inesi, 1985; Wakabayashi et al., 1990b), which binds MgATP (step 1) with high affinity (Dupont, 1980; Lacapere & Guillain, 1993). The interaction with MgATP triggers a conformational change, Ca_2·E1·MgATP to Ca_2·E1′·MgATP (step 2; Petithory & Jencks, 1986; Kubo et al., 1990; Coan & Keating, 1982; Lewis & Thomas, 1992), which activates the enzyme for ATP-dependent phosphorylation and formation

Scheme 1

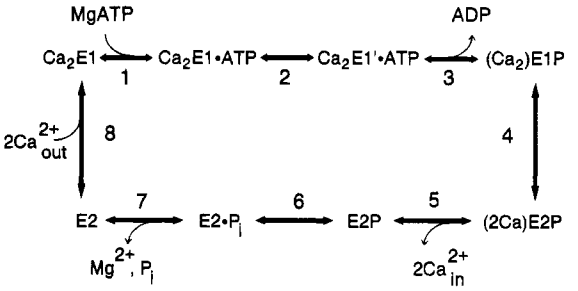

† This work was supported in part by grants to D.D.T. from the National Institutes of Health (GM27906 and AR39754) and a Grant-in-Aid to J.E.M. from the American Heart Association, Minnesota Affiliate.

* Author to whom correspondence should be addressed.
‡ University of Minnesota Medical School.
§ National Institute on Aging.

⊗ Abstract published in *Advance ACS Abstracts,* March 1, 1995.

[1] Abbreviations: SR, sarcoplasmic reticulum; NEM, *N*-ethylmaleimide; IASL, *N*-(1-oxyl-2,2,6,6-tetramethyl-4-piperidinyl)iodoacetamide; [^{2}H]IASL, perduterated form of IASL; MOPS, 3-morpholinopropanesulfonic acid; MES, 2-morpholinoethanesulfonic acid; ATP, adenosine 5′-triphosphate; EGTA, ethylene glycol bis(β-aminoethyl ether)-*N,N,N′,N′*-tetraacetic acid; ADP, adenosine 5′-diphosphate; AMPPCP, β,γ-methyleneadenosine 5′-triphosphate; caged ATP, P^3-1-(2-nitrophenyl)ethyl ester of ATP; PCA, perchloric acid; TCA, trichloroacetic acid; EPR, electron paramagnetic resonance; f_M, mole fraction of rotationally mobile spectral component; f_R, mole fraction of rotationally restricted spectral component.

0006-2960/95/0434-4864$09.00/0

of the ADP-sensitive phosphoenzyme, (Ca_2)E1P (step 3; Shigekawa et al., 1978; Shigekawa & Dougherty, 1978; Shigekawa & Kanazawa, 1982; Froehlich & Heller, 1985). Calcium translocation is associated with a rapid conformational change in the phosphoenzyme that converts (Ca_2)E1P to an ADP-insensitive form, (2Ca)E2P (step 4) and dramatically reduces its affinity for Ca^{2+} (Froehlich & Heller, 1985). This is followed by a slow reaction (step 5) in which Ca^{2+} is released into the SR lumen (Froehlich & Heller, 1985; Hanel & Jencks, 1991; Orlowski & Champeil, 1991). Rapid hydrolysis of ADP-insensitive E2P (step 6) yields E2·P_i (step 7; Kanazawa & Boyer, 1973; Froehlich & Taylor, 1975, 1976), which regenerates E1 via a sequence of reactions that impose rate limitation on the overall process. There is kinetic evidence that enzyme oligomers are involved in the transport mechanism (Froehlich & Taylor, 1976; Ikemoto et al., 1981a,b; Froehlich & Heller, 1985; Wang, 1986) and that dynamic changes in protein−protein interactions may play an important role in modulating some of the mechanistic steps (Bigelow et al., 1992; Karon & Thomas, 1993; Karon et al., 1994), but these points remain controversial (Thomas & Mahaney, 1993; Thomas et al., 1993; MacLennan et al., 1992; Inesi, 1990; Martonosi et al., 1990).

A variety of methods has demonstrated that conformational changes coincide with each specific step in the enzyme mechanism, including intermediate differences in sulfhydryl reactivity (Murphy, 1978; Yamada & Ikemoto, 1978), tryptic cleavage patterns (Vilsen & Andersen, 1987), the emissions of covalently attached fluorescent probes (Pick & Bassilian, 1981; Froud & Lee, 1986; Birmachu et al., 1989; Wakabayashi et al., 1990a), the intrinsic fluorescence of the ATPase (Dupont, 1976; Champeil et al., 1986), the infrared spectroscopic patterns (Arrondo et al., 1987), and the X-ray diffraction of the enzyme [reviewed by Blasie et al. (1990)]. In recent years, much attention has been focused on understanding the Ca^{2+}- and ATP-stimulated conformational change (Scheme 1, step 2) that activates the enzyme for ATP-dependent phosphoenzyme formation, including kinetic studies (Pierce et al., 1983; Inesi et al., 1990; Petithory & Jencks, 1986), spectroscopic analysis (Suzuki et al., 1987, 1989; Obara et al., 1988; Kubo et al., 1990; Blasie et al., 1990; Barth et al., 1990, 1991; Bigelow et al., 1992; Buchet et al., 1992), chemical cross-linking (Ross et al., 1991), and site-directed mutagenesis (MacLennan, 1990; MacLennan et al., 1992; Zang, 1993). The understanding of the physical basis by which this key conformational change initiates and drives the kinetics of Ca^{2+} translocation is an intriguing problem because it links structural changes associated with Ca^{2+} binding to the high-affinity transport sites, located in the transmembrane helix region of the protein, with structural changes associated with high-affinity ATP binding in the catalytic site, located more than 4 nm away in the cytoplasmic domain of the protein [Toyoshima et al., 1993; reviewed by Inesi et al. (1992); MacLennan et al., (1992)].

An especially valuable tool in the study of this particular conformational change has been electron paramagnetic resonance (EPR) spectroscopy using the iodoacetamide spin label IASL covalently attached to the enzyme specifically at Cys-674 (Wawrzynow et al., 1993). The effects of substrates and ligands on the IASL−Ca-ATPase spectrum have been extensively characterized by Coan and co-workers at 25 °C (Coan & Inesi, 1977; Coan et al., 1979, 1986; Coan & Keating, 1982; Coan, 1983; Chen et al., 1991) and by Lewis and Thomas (1992) at 4 °C. The EPR spectrum of the iodoacetamide spin-labeled enzyme (IASL−Ca-ATPase) at 4 °C in the absence of specific ligands is characteristic of probes in a single motional state, but the addition of certain nucleotides (e.g., ATP, ADP, CrATP, AMPPCP) promotes the formation of a second motional state, indicative of a population of probes with reduced mobility. The presence of micromolar calcium enhances these effects, but calcium alone has no effect on the spectrum. It has been demonstrated previously (Coan & Keating, 1982; Lewis & Thomas, 1992) that the two motional states of the spin label correspond to two distinct conformational states of the enzyme. The addition of inorganic phosphate (P_i) or the appliction of conditions that favor enzyme phosphorylation by P_i does not produce the restricted component in the EPR spectrum (Lewis & Thomas, 1992), indicating that the ATPase intermediates producing the strongly immobilized EPR signal, and thus the distinct enzyme conformation, are restricted to Ca_2·E1′·ATP and (Ca_2)E1P states. Correlation of the spectroscopic data (Coan & Inesi, 1977; Coan & Keating, 1982; Coan, 1983) with kinetic data (Petithory & Jencks, 1986; Inesi et al., 1990) suggests that the conformational change measured by IASL is the same as that that activates the enzyme for phosphorylation (Wawrzynow et al., 1993).

In a previous report, Lewis and Thomas (1992) described a time-resolved EPR method to study conformational transitions in the Ca-ATPase. Experiments were carried out at 4 °C to slow the enzyme conformational transients and thus improve spectroscopic resolution. Calcium pumping by the IASL−Ca-ATPase was initiated by laser flash photolysis of caged ATP [reviewed by McCray and Trentham (1989)], and EPR signals were monitored transiently with 1 s time resolution. The use of a long instrumental time constant (1 s) and multiple laser flashes (a 1 s burst of 50 pulses) was required for acquisition of the EPR transients (Berger et al., 1989; Fajer et al., 1990; Lewis & Thomas, 1991, 1992; Ostap & Thomas, 1991; Thomas et al., 1993), but these factors limited the spectral analysis to changes that occur on the 1 s time scale and in the steady state. Recent technological advances, including intense (150 mJ/cm^2), single-pulse (10 ns) laser flashes and millisecond instrumental time constants (Ostap et al., 1993), now allow us to monitor changes in the [^{2}H]IASL−Ca-ATPase spectrum during the pre-steady-state phase of Ca^{2+} translocation and, thus, study directly the conformational change that activates the enzyme for ATP-dependent phosphorylation.

Therefore, in the present study, we have paired time-resolved EPR measurements with rapid acid-quenching measurements of the enzyme's biochemical kinetics in order to quantitatively correlate conformational changes in the Ca-ATPase with specific steps in the enzyme mechanism. We find quantitative agreement between the rates of the EPR transient (i.e., transient conformational change) and enzyme phosphorylation, but only for a population of catalytic sites with delayed phosphorylation. The results are discussed in terms of a Ca-ATPase oligomer consisting of conformationally coupled subunits. The results provide new physical evidence correlating a specific conformational change with the activation of the Ca-ATPase for phosphorylation and suggest that the enzyme's oligomeric structure modulates ATP-dependent phosphorylation.

MATERIALS AND METHODS

Reagents and Solutions. The [^{2}H]IASL used in this study was a gift from Dr. Albert Beth (Vanderbilt University). ATP and MOPS were obtained from Sigma. Caged ATP and A23187 were obtained from Calbiochem. Other reagents, obtained from various sources, were of the highest purity available. All EPR and quenched-flow experiments were carried out at 2 °C in a buffer containing 5 mM $MgCl_2$, 0.45 mM $CaCl_2$, 0.5 mM EGTA (3.5 μM free Ca), 20 mM MOPS (pH 7.0) (henceforth denoted standard buffer), and variable [KCl] from 0.1 to 0.6 M as indicated.

Preparations and Assays. Sarcoplasmic reticulum (SR) vesicles were prepared from the fast-twitch skeletal muscle of New Zealand white rabbits (Fernandez et al., 1980). The vesicles were purified on a discontinuous sucrose gradient (Lewis & Thomas, 1992) to remove heavy SR vesicles (junctional SR containing calcium release proteins). Purified light and intermediate SR vesicles were harvested and then pelleted in 20 mM MOPS (pH 7.0). The pellets were resuspended in 0.3 M sucrose and 20 mM MOPS (pH 7.0) (henceforth denoted sucrose buffer), rapidly frozen, and stored in liquid nitrogen until use. All preparations were done at 4 °C. SR vesicles prepared in this fashion were typically 75% Ca-ATPase (7 nmol of Ca-ATPase/mg of SR) and contained approximately 80 mol of phospholipid/mol of Ca-ATPase (Bigelow et al., 1986). The ATP hydrolysis of the SR vesicles was fully coupled to calcium transport (Squier & Thomas, 1989). Calcium-dependent ATPase activity was measured as described by Squier and Thomas (1989). The molar concentration of phospholipids in SR and SR lipid extracts and samples was determined from phosphorus assays (Chen et al., 1956). SR protein concentrations were determined by the biuret assay (Gornall et al., 1949) using bovine serum albumin as a standard.

Caged ATP was purified by HPLC on a preparative Bio-Rad MA7Q anion-exchange column (2 × 10 cm) and eluted with a linear gradient of 0−2.0 M triethylamine bicarbonate (pH 7.8) (Berger & Thomas, 1991). The eluted caged ATP was then lyophilized, resuspended in distilled water, lyophilized again, and diluted to a final concentration of 50−100 mM in distilled water. The caged ATP concentration was determined spectrophotometrically at 260 nm, using ϵ_{260} = 18 900 M^{-1} cm^{-1}. The caged ATP solution was divided into small aliquots and stored at −20 °C until use.

The amount of ATP produced in the EPR samples by laser flash photolysis was determined in the following manner. After the EPR experiment, each sample (10−15 μL) was diluted 10-fold in water and centrifuged at 100000*g* for 15 min using a Beckman TL-100 ultracentrifuge, in order to pellet the SR vesicles. The supernatant was collected and placed in a 3 × 3 mm quartz cuvette, and the concentration of caged ATP remaining in the sample was calculated from the absorbance at 351 nm, using ϵ_{351} = 600 M^{-1} cm^{-1}. This wavelength was selected because neither ATP, ADP, nor any soluble SR proteins have any absorbance at this position. After spectrophotometric analysis, the amount of P_i in the sample was determined by the method of Lanzetta et al. (1979), using duplicate 50 μL sample aliquots. The change in [caged ATP] measured spectrophotometrically matched the amount of P_i in the samples to within 5%. Agreement between these two values justifies the assumption that the ATP liberated by the laser flash was completely hydrolyzed by the enzyme.

Spin Labeling the Ca-ATPase. The internal dynamics of the Ca-ATPase was monitored using the perdeuterated iodoacetamide spin label, *N*-(1-oxyl-2,2,6,6-tetramethyl-4-piperidinyl)iodoacetamide ([^{2}H]IASL), covalently bound to the ATPase ([^{2}H]IASL−Ca-ATPase) specifically at Cys-674 (Wawrzynow et al., 1993). SR vesicles were suspended to 10 mg/mL in sucrose buffer (pH 7.0) and prelabeled with 0.1 mM *N*-ethylmaleimide (NEM) for 30 min at 25 °C, which was required to block fast-reacting sulfhydryl groups (see Discussion). This was followed by the addition of 0.2 mM IASL. After a 3 h incubation at 25 °C, the sample was diluted with ice-cold sucrose buffer (pH 7.0), and unbound label was removed by washing the vesicles three times in sucrose buffer (pH 7.0) and centrifugation at 100000*g* for 30 min at 4 °C. After the last wash, the spin-labeled SR was resuspended to about 20 mg/mL in sucrose buffer (pH 7.0) and stored frozen in liquid nitrogen until use. The stoichiometry of label incorporation was 0.75 ± 0.1 mol of IASL/mol of Ca-ATPase (assuming 7 nmol of Ca-ATPase/mg of SR).

NEM preblocking and spin labeling the enzyme reduced enzymatic activity by about 30% compared to the control unlabeled enzyme. In a study comparing control SR with (a) NEM-preblocked SR (no spin label), (b) spin-labeled SR (no NEM preblock), and (c) NEM-preblocked and spin-labeled SR, we found that the NEM addition step was responsible for the loss of activity. The quenched-flow kinetic studies presented in the Results indicate that the reduction in activity arises from a 30% loss of active sites, with the remaining enzyme being kinetically unaffected (see Results). Freezing of the spin-labeled SR had no further effect on either Ca-ATPase activity or ATP-dependent phosphoenzyme formation rates or levels, and there was no effect on the conventional or transient EPR spectrum.

EPR Spectroscopy. Conventional and transient EPR spectra were acquired using a Bruker ESP 300 spectrometer equipped with a Bruker ER4102 ST cavity (TE_{102}) and were digitized with the spectrometer's built-in microcomputer using Bruker OS-9-compatible ESP 1620 spectral acquisition software. Conventional EPR spectra were obtained using 100 kHz field modulation (with a peak-to-peak modulation amplitude of 2 G), with a microwave field intensity (H_1) of 0.14 G, determined from peroxylaminedisulfonate calibrations (Squier & Thomas, 1986). Transient EPR spectra were obtained under the same conditions, except that the peak-to-peak modulation amplitude was set to 5 G. Conventional EPR spectra were acquired using a 100 G sweep width with a 164 ms dwell time and a 164 ms time constant. Transient EPR spectra were obtained at a single field position (sweep width, 0 G), defined by the restricted component in the low-field peak of the [^{2}H]IASL−SR spectrum (see Results), using a 10 ms filter time constant and a 10 ms dwell time. The sample concentration was 10 mg of SR/mL in all of the EPR experiments. Identical spectral results were obtained over a 20-fold concentration range (from 1 to 20 mg of SR/mL, data not shown), suggesting that vesicle concentration had no effect on the results. All EPR samples were contained in a 20 μL well on a homemade gas-permeable KEL-F cover plate affixed to a no-well quartz Suprasil tissue flat cell (Wilmad, Buena, NJ). The sample temperature was controlled to within 0.5 °C with a Bruker ER 4111 variable temperature controller. Sample temperature was monitored

using a Sensortek Bat-21 digital thermometer with an IT-21 thermocouple attached to the side of the sample holder. All spectra were recorded at 2 °C.

Caged ATP was photolyzed during EPR experiments using a single 10 ns flash at 351 nm from a XeF excimer laser (LPX200i, Lambda Physik, Acton, MA). The light was introduced directly to the sample through an optical port on the front of the EPR cavity. The dimensions of the KEL-F sample well were the same as those of the optical port on the EPR cavity, such that the entire sample was uniformly exposed to the laser flash. Light energy incident on the sample was ~150 mJ/cm^2 for a single pulse and typically resulted in 10% conversion of caged ATP to ATP. There was no detectable sample heating in response to the laser flash, and exposure of the ATPase to the laser light pulse had no detrimental effect on enzymatic activity, as determined by activity measurements on the sample before and after sample irradiation. Samples were exposed to only one laser flash each, in order to prevent complications from product build-up. The EPR transients from a series of identical samples (n = 9−25) were averaged, in order to produce transients with sufficient signal-to-noise ratios for curve fitting and analysis.

We tested whether the turbidity of the SR vesicles attenuated the laser light as it passed through the EPR sample (0.5 mm path length), which would result in an ATP concentration gradient through the sample during the transient EPR experiment. In this experiment, we used 10 mg/mL SR and 1 mM caged ATP suspended in standard buffer (pH 7.0) at 2 °C, and we measured the percent caged ATP photolyzed as a function of sample depth. The sample well depths selected were 0.2, 0.4, 0.6, 0.8, and 1.0 mm, the rationale being that the average [ATP] produced by a laser flash would correspond to sample depths of 0.1, 0.2, 0.3, 0.4, and 0.5 mm, respectively. We found no difference in the ATP concentration (0.1 ± 0.01 mM) produced at each sample depth, indicating that the SR vesicles imposed no light gradient through the EPR sample. Therefore, the only attenuation of the incident laser light was that absorbed by the caged ATP at 351 nm, and even this was negligible (A_{351} = 0.03).

EPR Spectral Analysis. Conventional EPR spectra were downloaded to an IBM-compatible microcomputer and analyzed with software developed in our laboratory by Robert L. H. Bennett. EPR transients were fit to a lag function:

$$I(t) = A_0\{1 + [1/(k_2 - k_1)][k_2 e^{-k_1 t} - k_1 e^{-k_2 t}]\} \quad (1)$$

using a program (KFIT) written by N. C. Millar. The fit yielding the highest correlation coefficient, R, was selected. Conventional EPR spectra were normalized to the same number of spins by dividing each spectrum by its double integral. Transient EPR spectra were normalized for modulation amplitude and to the same number of spins by dividing by the double integral of the corresponding conventional EPR spectrum obtained prior to caged ATP photolysis.

Spectra subtractions were performed as described by Lewis and Thomas (1992). The control spectrum of [^{2}H]IASL−Ca-ATPase in buffer was chosen as one end point (designated the mobile component), and the other end point (designated the restricted component) was reached by subtracting the mobile component from the composite spectrum ([^{2}H]IASL−Ca-ATPase in standard buffer + nucleotide) in fractional increments: C − f_MM = R, where C, M, and R denote the composite, mobile, and restricted spectra, respectively, and f_M is the mole fraction of the mobile component. The restricted component end point was reached when the low-field peak of the difference spectrum was symmetrical, as required by EPR theory (Freed, 1976). The mole fraction of the restricted component (f_R) is simply 1 − f_M. Further details about the spectral subtraction procedure, including the assumptions made, are discussed in Lewis and Thomas (1992).

ATP-Dependent Phosphoenzyme Formation. Rapid mixing studies were performed as described by Froehlich and Heller (1985) using a quenched-flow apparatus driven by a stepping motor and equipped with Berger ball mixers. All rapid mixing experiments were performed at 2 °C, accomplished by moving the mixing device into a cold room. Unless otherwise indicated, the enzyme- and substrate-containing syringes both contained 0.1 M KCl, 5 mM $MgCl_2$, 0.45 mM $CaCl_2$, 0.5 mM EGTA, and 20 mM MOPS (pH 7.0). Phosphoenzyme formation was initiated by mixing SR vesicles (0.5 mg/mL), permeabilized by the calcium ionophore A23187 (1 μg/0.05 mg of SR), with an equal volume of the substrate medium containing 0.2 mM [γ-^{32}P]ATP and terminated after a variable time delay (4−800 ms) by the addition of 3% perchloric acid + 2 mM H_3PO_4 (final concentrations). The quenched vesicles were pelleted by centrifugation for 10 min at 3000g and 4 °C and then washed three times by similar centrifugation using a solution of 5% trichloroacetic acid, 6% polyphosphoric acid, 4 mM H_3PO_4, and 5 mM cold ATP. Pellet recovery following washing was greater than 95%. The final pellets were dissolved in 1 N NaOH overnight, and the ^{32}P-labeled phosphoenzyme was assayed by counting the Cerenkov radiation.

Dephosphorylation of the Phosphoenzyme by ADP. ADP dephosphorylation experiments were carried out as described previously by Froehlich and Heller (1985). SR vesicles (0.375 mg/mL) were phosphorylated at 2 °C (as described above) for a preset time t, and dephosphorylation by ADP was initiated by mixing 2 vol of the phosphorylation reaction mixture with 1 vol of a solution containing 5 mM ADP, 100 mM KCl, 5 mM $MgCl_2$, 0.45 mM $CaCl_2$, 0.5 mM EGTA, and 20 mM MOPS (pH 7.0) to provide a final [ADP] of 1.66 mM after mixing. After a variable time delay, the dephosphorylation reaction was terminated as before, and the vesicles were processed and assayed for ^{32}P-containing enzyme. In the calcium jump experiments, the dephosphorylation medium contained 15 mM $CaCl_2$ and no EGTA to provide a final [$CaCl_2$] of 5 mM after mixing.

Separation and Analysis of $^{32}P_i$ in the Presence of [γ-^{32}P]-ATP. [^{32}P]P_i liberation during ADP dephosphorylation was assayed according to Sumida et al. (1980). One milliliter of quenched sample was added to 1 mL of a 2% aqueous charcoal slurry. The sample was vortex mixed and centrifuged for 10 min at 3000g and 4 °C. One milliliter of the supernatant was added to another 1 mL of a 2% aqueous charcoal slurry, vortex mixed, and centrifuged as before. One milliliter of the supernatant from the second centrifugation was added to 1.5 mL of water saturated with 1:1 isobutyl alcohol/xylene contained in a 60 × 125 mm screw cap tube and vortex mixed. For quench solutions not containing any P_i, 50 μL of (non-radioactive) 10 mM K_2HPO_4 was added for color development in the next step. To each tube was added 0.8 mL of 5% ammonium molybdate (in 4 N HCl)

reagent, the tubes were capped, and the samples were vortex mixed briefly. Complexation between P_i and the molybdate was allowed to proceed for 15 min. Following the incubation, 4 mL of water-saturated 1:1 isobutyl alcohol/xylene was added to each tube, and the tubes were capped and vortex mixed 3 × 10 s, with 10 s in between mixing. The phases were allowed to separate for 10 min, after which 2 mL of the organic (upper) phase was pipeted into 5 mL of 1 N NaOH contained in a scintillation vial. The vials were capped and shaken to remove the color and assayed for ^{32}P by counting the Cerenkov radiation.

Dephosphorylation of the Phosphoenzyme by EGTA. In a hand mixing experiment, SR vesicles (0.25 mg/mL) were phosphorylated at 2 °C using 0.1 mM [γ-^{32}P]ATP in SRB (pH 7.0) in the presence of calcium ionophore A23187 (1 μg/ 0.05 mg of SR) for 20 s, followed by mixing 2 vol of the phosphorylation reaction mixture with 1 vol of a solution containing 100 mM KCl, 5 mM $MgCl_2$, 15 mM EGTA, and 20 mM MOPS (pH 7.0). After a variable time delay, the phosphoenzyme decay reaction was terminated as before, and the vesicles were processed and assayed for ^{32}P-containing enzyme as described earlier.

Phosphoenzyme Formation from P_i. In a hand mixing experiment, SR vesicles (0.25 mg/mL) were phosphorylated at 2 °C in a solution containing 4 mM [^{32}P]Na_2HPO_4, 5 mM $MgCl_2$, 2 mM EGTA, and 20 mM MES (pH 6.0) for 15 min, after which the reaction was terminated, and the vesicles were processed and assayed for ^{32}P-containing enzyme.

Curve Fitting and Kinetic Modeling. The selection of an appropriate model function for the pre-steady-state behavior of the phosphorylation reaction was carried out using the Marquardt−Levenberg-based curve-fitting routines contained in the program MLAB (Knott, 1979). Mono- and biexponential functions of the form,

$$[EP]_t = A_i\{1 - e^{-k_i t}\} \quad (i = 1, 2) \qquad (2)$$

were tested, and the best fit was chosen on the basis of optimization of the determination coefficient, R^2, and minimization of the difference between the fitted curve and data points (sum-of-squares error). The amplitude (A_i) and rate (k_i) parameters were constrained to positive numbers and allowed to vary without bound. In the case where a biexponential function showed no improvement over a monoexponential fit, the program generated gave identical amplitude (A_i) and rate (k_i) parameters for the two phases.

RESULTS

EPR Spectrum of [^{2}H]IASL−Ca-ATPase. Internal rotational motions of the Ca-ATPase were measured using the iodoacetamide spin label IASL, which has been shown to be quite specific for Cys-674 on the enzyme (Wawryznow et al., 1993). In the present study, the perdeuterated derivative of IASL ([^{2}H]IASL) was used to enhance peak resolution in the spectrum, as demonstrated previously (Lewis & Thomas, 1992). The EPR spectrum of the iodoacetamide spin-labeled Ca-ATPase ([^{2}H]IASL−Ca-ATPase) at 2 °C is shown in Figure 1. Apart from a minor (less than 5%) contribution from weakly immobilized spin probes (peak A, Figure 1), the spectrum consists of at least two components, the mole fractions (f) of which depend on the presence of nucleotide (Lewis & Thomas, 1992; Coan et al., 1979, 1986; Coan, 1983; Coan & Keating, 1982; Coan & Inesi, 1977). In the presence of 5 mM $MgCl_2$, 0.45 mM $CaCl_2$, 0.5 mM EGTA, and 20 mM MOPS (pH 7.0) (denoted standard buffer) with 100 mM KCl, the spectrum primarily consists of a single rotationally mobile component (peak B, $f_M \approx 0.95$, $2T_{\parallel}' = 52 \pm 0.25$ G), although there is evidence of a minor, more restricted component (peak C, $f_R \approx 0-5\%$), seen as shoulders on the low- and high-field peaks of the primary component. The spectrum is identical in a medium containing 0.3 mM sucrose and 20 mM MOPS (pH 7.0), and [KCl] has no effect on the spectrum up to 0.6 M. Upon the addition of ATP, ADP, or ATP analogs (AMPPNP, AMPPCP), the mole fraction of the restricted spectral component (peak C, $2T_{\parallel}' = 63 \pm 0.5$ G) increases at the expense of the mole fraction of the more mobile primary component (peak B). This effect is enhanced by the presence of micromolar calcium, but calcium alone (i.e., in the absence of nucleotide) has no effect (Lewis & Thomas, 1992). Millimolar levels (1−5 mM) of ATP analogs (AMPPCP, AMPPNP) promote the greatest change in the mole fraction of restricted probes ($\Delta f_R \approx 0.50 \pm 0.025$), whereas equivalent

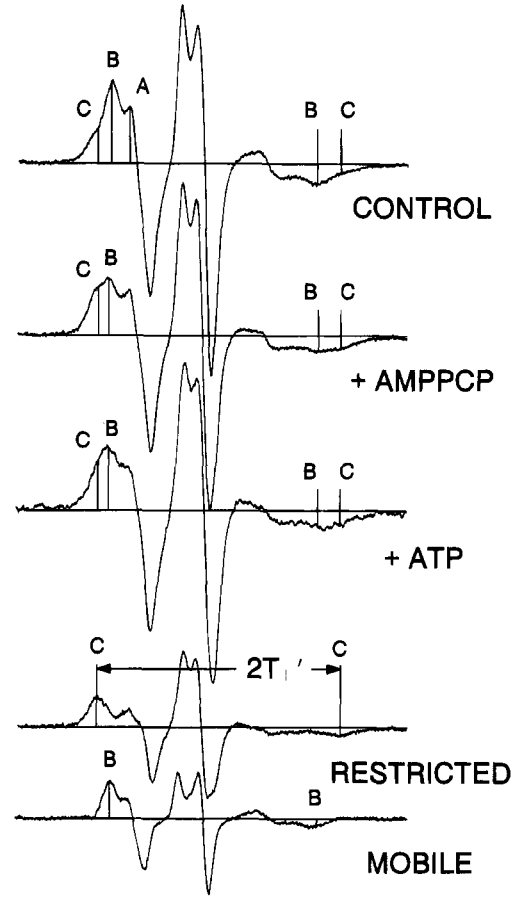

FIGURE 1: Effect of AMPPCP and ATP on the steady-state EPR spectrum of [^{2}H]IASL−Ca-ATPase. Spin-labeled enzyme (10 mg of SR/mL) was suspended in standard buffer containing 100 mM KCl (pH 7.0) and either no nucleotide (top), 5 mM AMPPCP (second), or 1 mM ATP (third) obtained immediately after the photolysis of caged ATP (see text). Spectra were recorded at 2 °C and are normalized to correspond to the same number of spins. The restricted (fourth) and mobile (fifth) component spectra were obtained by spectral subtraction (see Materials and Methods). Line height parameters denote probe populations that are weakly immobilized (A), rotationally mobile (B), and rotationally restricted (C). The spectral splitting ($2T_{\parallel}'$) is defined for the restricted component. Baselines represent 100 G.

Table 1: Effect of [AMPPCP] on the Mole Fraction of the Restricted Spectral Component (f_R) in the [^{2}H]IASL−Ca-ATPase Spectrum at 2 °C[a]

[AMPPCP] (mM)	f_R	normalized
0	0	0
0.01	0.07 ± 0.025	0.14
0.025	0.125 ± 0.025	0.25
0.05	0.2 ± 0.025	0.40
0.1	0.275 ± 0.025	0.55
0.25	0.35 ± 0.025	0.70
0.5	0.4 ± 0.025	0.80
1.0	0.45 ± 0.025	0.90
5.0	0.5 ± 0.025	1.00

[a] Mole fraction of restricted probes was obtained by spectral subtraction as described in Materials and Methods. f_R values are the average of two separate measurements, and the errors represent the difference between the two measurements.

amounts of ATP or ADP promote smaller changes ($\Delta f_R \approx 0.35 \pm 0.03$). Coan and co-workers (Coan & Keating, 1982; Coan 1983; Coan et al., 1986) have shown that the spectral change arises from the conformational change associated with enzyme activation by nucleotide binding to the active site of the enzyme, in the presence of calcium (i.e., Ca_2•E1 to Ca_2•E1′•nucleotide).

The nucleotide concentration dependence of f_R was examined by titrating the restricted component in the EPR spectrum with the nonhydrolyzable ATP analog AMPPCP (Table 1). Even at low concentrations, AMPPCP increases the mole fraction of restricted probes (see Table 1), suggesting that the appearance of the restricted component is related to high-affinity nucleotide binding. In fact, fitting the data in Table 1 with a binding equation (not shown) indicated two independent nucleotide dissociation constants, 50 and 650 μM, in a ratio of 3:1.

Using the γ,β-bidentate form of chromium ATP (CrATP), Chen et al. (1991) demonstrated that the nucleotide-induced spectral change is conserved upon enzyme phosphorylation and calcium occlusion at 37 °C. In the present study, we also found that the spectrum of chromium-inactivated [^{2}H]-IASL−Ca-ATPase in standard buffer at 2 °C (Figure 2) is identical to that obtained in the presence of nucleotides (Figure 1), indicating that the observed conformational transition is conserved during enzyme phosphorylation and calcium occlusion at 2 °C. In contrast, those ligands and buffer conditions that promote the formation of the enzyme intermediate state E2 (e.g., 5 mM EGTA + 40 mM MES (pH 6.2) and thapsigargin) or that favor enzyme phosphorylation by P_i (e.g., 2 mM EGTA, 10 mM $MgCl_2$, 4 mM NaH_2PO_3, and 20 mM MES (pH 6.0)) have no significant effect on the spectrum at 2 °C (Figure 2). It is possible that the small amount of E2P that forms from P_i at 2 °C (0.13 ± 0.03 nmol/mg) prevents the detection of an E2P contribution to the restricted component (peak C, Figure 2), but this is unlikely. Coan (1983) has demonstrated that the principal effect of enzyme phosphorylation by P_i at 25 °C (typical EP levels of 1−1.2 nmol/mg) is to broaden slightly the low-field peak of the IASL−Ca-ATPase spectrum, but this effect is dependent on the presence of 40% dimethyl sulfoxide (DMSO), which enhances phosphorylation by P_i. Lewis and Thomas (1992) obtained a similar result at 4 °C, but also reported that 40% DMSO alone produced nearly all of the observed spectral effects, suggesting that the small P_i-induced conformational states formed in the presence of DMSO do not correspond to the normal intermediates in the cycle. Therefore, having found no change in the EPR spectrum of the [^{2}H]IASL−Ca-ATPase stabilized in any E2 form, we suggest that the observed conformational change induced by nucleotide binding and enzyme phosphorylation is reversed upon phosphoenzyme isomerization from (Ca_2)E1P to (2Ca)-E2P at 2 °C.

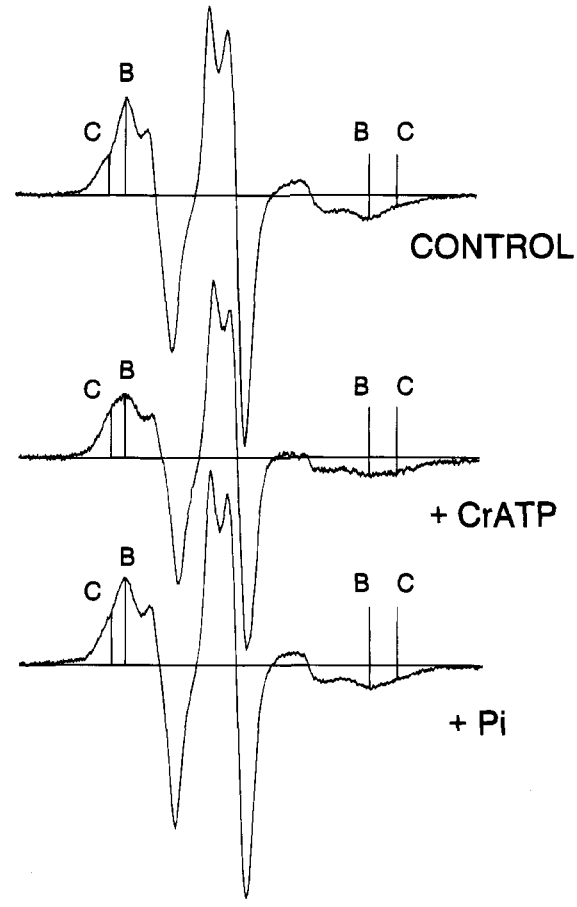

FIGURE 2: Effect of CrATP and P_i on the steady-state EPR spectrum of [^{2}H]IASL−Ca-ATPase. Spin-labeled enzyme (10 mg of SR/mL) either (top) suspended in standard buffer containing 100 mM KCl (pH 7.0) in the absence of nucleotide or in P_i (middle) in the same buffer following preincubation with 5 mM CrATP for 90 min at 37 °C or (bottom) following preincubation with 4 mM Na_2HPO_4, 10 mM $MgCl_2$, 2 mM EGTA, and 20 mM MES (pH 6.0) for 15 min at 25 °C. The corresponding control spectrum in the absence of P_i obtained at pH 6.0 (not shown) did not significantly differ from that obtained at pH 7.0. Spectra were obtained at 2 °C and are normalized to correspond to the same number of spins. Line height parameters are defined in the legend to Figure 1. Baselines represent 100 G.

Transient EPR of [^{2}H]IASL−Ca-ATPase. The transition between the two conformational states during the transient phase of enzymatic cycling was monitored by detecting changes in the EPR signal as a function of time after the photolysis of caged ATP in the EPR sample, with a time resolution of 10 ms (Figure 3). Transient EPR experiments were carried out at 2 °C in order to slow the kinetics of the enzyme and to maximize the effects of substrates on the spectrum. The EPR signal was monitored at a single position in the low-field region of the spectrum (peak C, Figure 1), which is the region of maximum sensitivity to the nucleotide-induced change in the EPR spectrum (Lewis & Thomas, 1992). Prior to photolysis, the intensity at this field position was identical to the intensity of peak C in the no-nucleotide

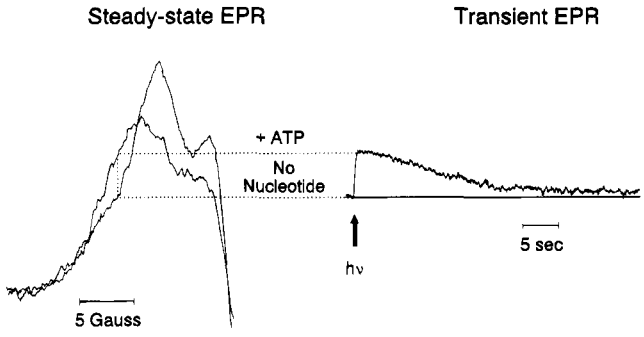

FIGURE 3: Steady-state and transient EPR spectra of [^{2}H]IASL−Ca-ATPase (10 mg of SR/mL) in standard buffer containing 100 mM KCl (pH 7.0) at 2 °C. (Left) Overlays of the low-field portions of the steady-state spectra of [^{2}H]IASL−Ca-ATPase in the absence or presence of 0.1 mM ATP. The spectral intensity of the steady-state spectrum was monitored at a single position (vertical dashed line) during transient EPR experiments. (Right) Transient EPR spectrum. At time zero (denoted by the arrow), a laser pulse directed into the EPR cavity liberated 0.1 mM ATP in the sample. Control experiments in the absence of caged ATP indicated no significant effect of the laser pulse itself on the EPR signal intensity. The no-nucleotide steady-state spectrum was obtained by signal-averaging four scans on a single sample, the +ATP steady-state spectrum was obtained as a single scan, and the transient EPR spectrum is the average of 16 individual transients obtained using separate samples.

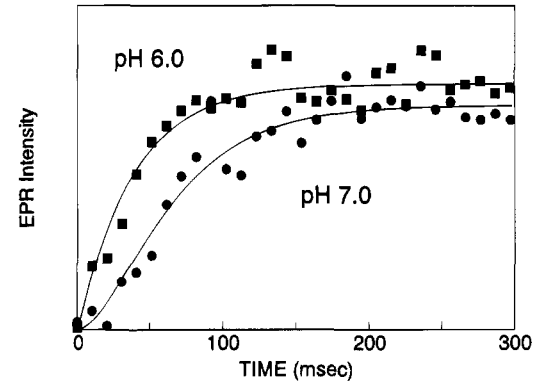

FIGURE 4: Effect of pH on the transient EPR spectrum at 2 °C. [^{2}H]IASL−Ca-ATPase (10 mg of SR/mL) was suspended in 100 mM KCl, 5 mM $MgCl_2$, 0.45 mM $CaCl_2$, 0.5 mM EGTA, 1 mM caged ATP, and either 20 mM MOPS (pH 7.0) (●) or 20 mM MES (pH 6.0) (■). At time zero, 0.1 mM ATP was generated in the EPR sample by laser flash photolysis. The EPR transients were best fit (solid lines) by a lag function (see Materials and Methods), with exponential formation rates of 20 ± 2 s^{-1} (mean ± SD) at pH 7.0 and 22 ± 1 s^{-1} (mean ± SD) at pH 6.0. Control experiments in the absence of caged ATP at both pH levels indicated no significant effect of the laser pulse itself on the EPR signal intensity. Transient EPR spectra are the average of nine individual transients obtained using separate samples.

sample (Figure 3, lower dashed line). The liberation of 100 μM ATP (arrow) in the presence of micromolar calcium produced a rapid rise in the EPR signal intensity to the level of peak C in the ATP spectrum (Figure 3, upper dashed line), indicating an ATP turnover-induced increase in the population of less mobile probes. The signal maintained a steady-state level during enzyme cycling, which lasted about 5 s. The length of the steady-state phase matched the expected duration calculated using the ATPase turnover rate at 2 °C and 0.1 mM ATP (about 0.1 μmol·mg^{-1}·min^{-1}) and SR concentration (10 mg/mL). When the ATP was depleted, the signal intensity decreased to a level that was slightly greater than the original intensity prior to ATP liberation (peak C, no-nucleotide spectrum). The increase in the final intensity level is consistent with effects of 0.1 mM ADP on the no-nucleotide spectrum (see above). The EPR intensity always returned to the original level, provided each sample was exposed to a single laser flash. For samples exposed to successive laser flashes, the increased ADP in the sample resulted in a progressive increase in the restricted component in the no-nucleotide spectrum, such that there was little difference between the no-nucleotide and ATP spectra at peak C. This quickly decreased the amplitude of the EPR transient to the noise level of the measurement. Therefore, each sample analyzed was exposed to a single laser flash, and transients from 16−25 individual samples were averaged to improve the signal-to-noise ratio in the transient EPR spectrum.

The time base of the EPR transient in Figure 3 has been expanded to show the changes in the EPR intensity during the pre-steady-state phase of ATP hydrolysis (Figures 4−6). Each point was acquired with a 10.24 ms dwell time and a 10.24 ms filter time constant. The 10 ns laser pulse of 351 nm light occurred at time zero. As shown in Figure 4, in the presence of standard buffer (pH 7.0) containing 0.1 M KCl, the signal exhibited a brief lag followed by a monoexponential increase (see Materials and Methods) with a rate of 21 ± 2 s^{-1}. The amplitude of the EPR transient corresponded to a mole fraction (f_R) of 0.35 ± 0.03, indicating that the steady-state population of enzyme units having a spin label with restricted mobility was about 35%. This is smaller than the value obtained using saturating AMPPCP (5 mM), which restricted the mobility of 50% of the probes (f_R = 0.50 ± 0.025, see above), consistent with the steady-state EPR results described earlier.

The photolysis rate of caged ATP at 2 °C in pH 7.0 buffer has been previously reported to be about 25 s^{-1} (Barabás & Keszthelyi, 1984), and the presence of millimolar $MgCl_2$ is expected to decrease this rate approximately 2-fold (Walker et al., 1988). To determine the effect of the kinetics of caged ATP photolysis on the rate of the EPR transient under our experimental conditions, we recorded the transient EPR spectrum at pH 6.0 (5 mM $MgCl_2$, 0.45 mM $CaCl_2$, 0.5 mM EGTA, 20 mM MES (pH 6.0), and 0.1 mM KCl), where the photolysis rate of caged ATP is an order of magnitude faster than that at pH 7.0 (Barabás & Keszthelyi, 1984; Walker et al., 1988), but phosphorylation kinetics is the same (see below). Lowering the pH from 7 to 6 eliminated the lag phase of the transient, but affected neither the exponential formation rate (22 ± 2 s^{-1}) nor the maximum amplitude of the EPR transient (Figure 4). This suggests that the rate of the EPR transient at pH 7 is not affected by the rate of ATP release from caged ATP. This is supported by the quenched-flow experiments described in the following section.

It has been demonstrated that [KCl] is an effective modulator of Ca-ATPase kinetics (Shigekawa et al., 1978; Shigekawa & Dougherty, 1978; Shigekawa & Kanazawa, 1982; Wakabayashi et al., 1986). To determine the effect of [KCl] on the transient EPR spectrum, we recorded transients using standard buffer (pH 7.0) over a range of [KCl]. The apparent rate of the EPR signal rise as a function of [KCl] is shown in Table 2, and the transient EPR spectra obtained in the presence of 0.1 and 0.4 M KCl are shown in Figures 5 (top) and 6 (top). In the absence of KCl, the rate of the EPR signal rise (22 ± 3 s^{-1}) was nearly identical to that observed at 0.1 M KCl (21 ± 2 s^{-1}). There was no

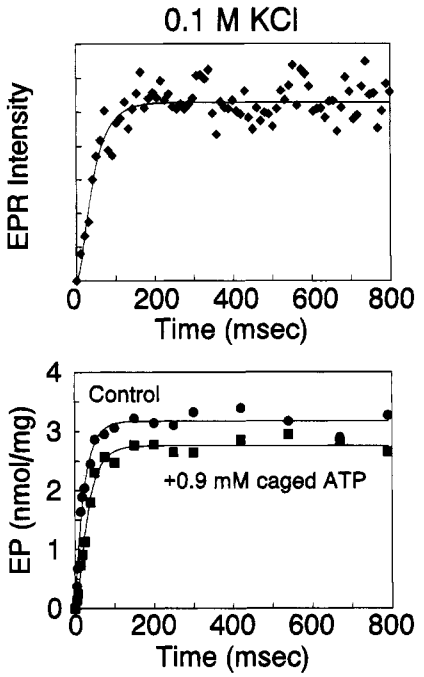

FIGURE 5: Comparison of the transient EPR spectrum with the pre-steady-state time course of ATP-dependent phosphoenzyme formation in SR vesicles at 2 °C in the presence of 0.1 M KCl: (top) transient EPR time course (◆), and (bottom) EP formation in untreated SR vesicles either without added caged ATP (●) or in the presence of 0.9 mM caged ATP (■). The EPR transient is the same as that shown in Figure 4 (pH 7.0 trace), but over a longer time course. For EP formation, SR vesicles (0.25 mg/mL) were phosphorylated by 0.1 mM [γ-^{32}P]ATP in standard buffer containing 100 mM KCl (pH 7.0). At the indicated times, the reaction was terminated by the addition of 3% perchloric acid + 2 mM H_3PO_4. The curves represent the best fits to the data using the parameters listed in Table 3.

Table 2: Effect of [KCl] on EPR Transient Formation Rates[a]

[KCl] (M)	k_2 (s^{-1})
0	22 ± 3
0.1	21 ± 2
0.2	18 ± 2
0.3	10 ± 1
0.4	6 ± 0.5
0.6	4 ± 0.5

[a] The EPR transient was best fit by a lag function as described in Materials and Methods. Errors represent the standard deviations of no less than four separate measurements.

difference in the lag phase or amplitude in the two transients, but the steady-state and decay phases were prolonged substantially in the absence of KCl relative to the presence of 0.1 M KCl (data not shown), consistent with previous reports describing K^+ activation of ATPase turnover rates (Shigekawa et al., 1978; Shigekawa & Dougherty, 1978; Wakabayashi et al., 1986). Increasing [KCl] beyond 0.1 M decreased the formation rate of the EPR transient, with the largest change in rate occurring between 0.2 M (18 ± 2 s^{-1}) and 0.4 M (6 ± 0.5 s^{-1}), where the rate decreased by a factor of 3. Over this range of [KCl], the lag phase of the EPR transient increased slightly and the amplitude of the transient decreased slightly, but there was no discernible change in the steady-state duration or decay phase (not shown). The EPR transient rise obtained in the presence of 0.6 M KCl was virtually identical to that obtained at 0.4 M KCl, except for a slightly slower rise rate (4 ± 0.5 s^{-1}).

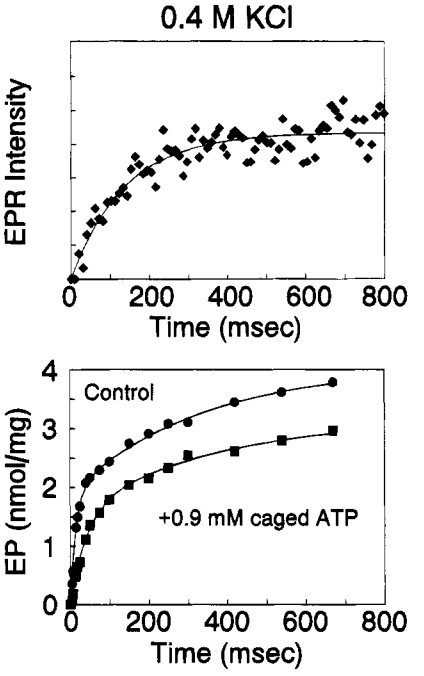

FIGURE 6: Comparison of the transient EPR spectrum with the pre-steady-state time course of ATP-dependent phosphoenzyme formation in SR vesicles at 2 °C in the presence of 0.4 M KCl: (top) transient EPR time course (◆) and (bottom) EP formation in untreated SR vesicles either without added caged ATP (●) or in the presence of 0.9 mM caged ATP (■). Transient EPR spectrum was obtained as described for Figure 3 using standard buffer containing 400 mM KCl (pH 7.0). For EP formation, SR vesicles (0.25 mg/mL) were phosphorylated by 0.1 mM [γ-^{32}P]ATP in standard buffer containing 400 mM KCl (pH 7.0). The curves represent the best fits to the data using the parameters listed in Table 3.

Table 3: Phosphoenzyme Formation Fit Parameters[a]

	A_1 (nmol/mg)	k_1 s^{-1}	A_2 (nmol/mg)	k_2 (s^{-1})
low [KCl] (100 mM)				
control	2.64	48.9	0.49	20.2
NEM + SL	1.60	54.2	0.68	20.1
+caged ATP[b]	2.98	27.4		
EPR signal	0.53	400	1.05	21
high [KCl] (400 mM)				
control	2.01	57.9	2.13	2.7
NEM + SL	1.50	51.2	1.02	5.2
+caged ATP[b]	1.70	21.0	1.77	1.9
EPR signal	0.46	16.7	1.46	5.3

[a] ATP-dependent EP formation data were fit with the function, $EP(t) = \sum_{n=1}^{n} A_n(1 - e^{-k_n t})$, where $n = 1$ (monoexponential) or $n = 1, 2$ (biexponential). The time-dependent EPR intensity ($I(t)$) was modeled using the function, $I(t) = A_0(1 + A_1e^{-k_1 t} - A_2e^{-k_2 t})$, where $A_0 = 1$ (arbitrary units), $A_1 = k_2/(k_1 - k_2)$, and $A_2 = k_1/(k_1 - k_2)$. The fit yielding the highest correlation coefficient, R, was selected. [b] Enzyme was not NEM-preblocked or spin-labeled.

ATP-Dependent Phosphoenzyme Formation at 2 °C. We performed acid quenched-flow experiments at 2 °C in order to obtain rate constants for the intermediate reactions of the enzyme cycle under the conditions of the EPR experiment. The goal of these studies was to identify the step in the enzyme mechanism associated with the transient conformational change detected by the EPR spin probe triggered by ATP release. The temperature of the EPR experiment was set at 2 °C in order to achieve adequate temporal resolution of the EPR transient. This required moving the quenched-flow apparatus to a cold room maintained at 2 ± 1 °C to ensure adequate temperature control of the mixers and

interconnecting capillary tubing (Froehlich et al., 1976). A second objective was to determine whether the presence of caged ATP or modification of the enzyme with *N*-ethylmaleimide (NEM) and [^{2}H]IASL influences the kinetic behavior of the Ca^{2+}-ATPase partial reactions.

The upper curve in Figure 5 (lower panel) depicts the time course of phosphorylation produced by mixing SR membrane vesicles (0.5 mg of protein/mL) in standard buffer medium with an equal volume of an identical solution containing 200 μM [γ-^{32}P]ATP and no enzyme. In this and all subsequent experiments, A23187 was present in the enzyme suspension in order to prevent Ca^{2+} accumulation in the vesicles. At 2 °C, ^{32}P incorporation displayed apparent monoexponential behavior; curve fitting with a rising monoexponential function gave a rate constant of 43.3 s^{-1}. To simulate the conditions of the EPR experiment, this measurement was repeated in the presence of 900 μM caged ATP, corresponding to a situation in which 10% of the caged ATP is photolyzed to ATP. The enzyme was preincubated with 1 mM caged ATP in standard buffer for several minutes and then mixed with sufficient ATP and caged ATP to give final concentrations of 100 and 900 μM, respectively. Unlike the EPR experiment, where the release of ATP is time-dependent, the increase in [ATP] produced by rapid mixing was virtually instantaneous. In the presence of 900 μM caged ATP, the rate of phosphorylation was reduced from 43.3 to 27.4 s^{-1}, while the maximum amount of ^{32}P incorporation was decreased by 5.1% compared to the control. Closer inspection of the time course revealed the presence of an initial lag phase, which delayed the onset of rapid ^{32}P labeling. These effects suggest that caged ATP weakly binds to the catalytic site during the preincubation and inhibits ATP binding from solution. Chemical analysis of the caged substrate by HPLC revealed the presence of a single, chromatographically pure chemical species. This suggests that the reduced level of phosphorylation detected in the presence of caged ATP is not due to ^{31}P incorporation from an ATP contaminant in the caged ATP during the incubation period prior to mixing.

The rate constant for caged ATP photolysis is dependent on pH, increasing linearly with [H^+] (Barabás & Keszthelyi, 1984; Walker et al., 1988). As shown in the previous section, lowering the pH from 7 to 6, while eliminating the lag phase from the EPR transient, did not affect the rate of rise of the signal. This implies that the ATPase partial reaction(s) producing the EPR signal should be insensitive to this change in pH. Because the strongly immobilized EPR signal is triggered by nucleotide binding (see above), we tested whether the reactions involved in ATP binding and enzyme phosphorylation were sensitive to variations in pH over this range.

Quenched-flow experiments were carried out at pH 6 and 7, measuring the time dependence of phosphorylation at different ATP concentrations. Phosphoenzyme formation was assayed at five time points ranging from 7 to 420 ms, and the rate constant, k_{app}, was evaluated from the best straight line fit to a semilog plot of [EP] vs time. The plot of k_{app} vs [ATP] in Figure 7 (Scheme 2), which was constructed from data collected at pH 7 (3−10 μM ATP) and pH 6 (12.5−100 μM), approximates a saturation curve with a maximum at or slightly above 100 μM. At pH 6 and 100 μM ATP, the apparent rate of phosphorylation was 42.8 s^{-1}, in excellent agreement with the value obtained at pH 7

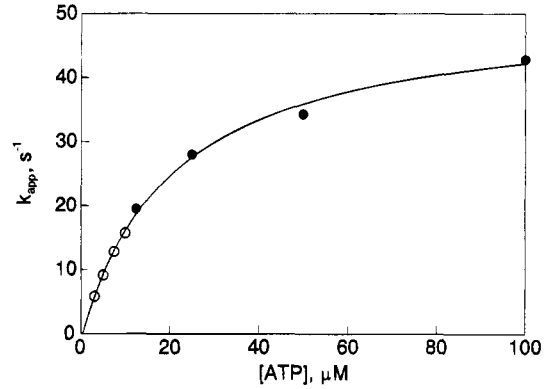

FIGURE 7: Effect of [ATP] on the apparent rate of phosphorylation at pH 6.0 and 7.0. SR vesicles (0.25 mg/mL) were phosphorylated with the indicated concentrations of [γ-^{32}P]ATP in a medium containing 0.1 M KCl, 5 mM $MgCl_2$, 0.45 mM $CaCl_2$, 0.5 mM EGTA, and either (●) 20 mM MOPS (pH 7.0) or (○) 20 mM MES (pH 6.0). The line represents the best fit of the data to the two-step model in Scheme 2 using the equation, $k_{app} = (p - q)/2$, $p = (k_1[ATP] + k_{-1} + k_2)$, and $q = (p^2 - 4k_1[ATP]k_2)^{1/2}$, where k_{app} is the apparent rate of phosphorylation and the rate constants, k_i, are defined in Scheme 2. The best fit was obtained using the rate constants $k_1 = 6.46 \times 10^6$ M^{-1} s^{-1}, $k_{-1} = 100$ s^{-1}, and $k_2 = 48.6$ s^{-1}.

Scheme 2

$$Ca_2 \bullet E1 + MgATP \underset{k_{-1}}{\overset{k_1}{\longleftrightarrow}} Ca_2 \bullet E1 \bullet MgATP \xrightarrow{k_2} (Ca_2)E1P + ADP$$

(43.3 s^{-1}). This implies that the rate constant for phosphorylation [or the conformational transition preceding phosphorylation (Petithory & Jencks, 1986)] is insensitive to pH, because at this substrate level ATP binding at the catalytic site is not rate-limiting (for phosphorylation). At subsaturating [ATP], k_{app} is strongly influenced by substrate binding and dissociation. The close approximation of the data points in Figure 7 to a single continuous function implies that these reactions are also insensitive to pH in this range.

We examined the effect of labeling the enzyme with NEM and [^{2}H]IASL on the kinetics of phosphorylation. Since SR contains several protein species (in addition to the Ca-ATPase) that have reactive sulfhydryl groups, pretreatment of the SR vesicles with NEM was essential to achieve specific labeling of the Ca-ATPase with [^{2}H]IASL at residue Cys-674 (Wawrzynow et al., 1993). To test whether any of these reactive sulfhydryls are essential for enzymatic activity, we measured phosphoenzyme formation using enzyme that had been preblocked with NEM and spin-labeled as described in Materials and Methods. Figure 8 compares the time courses of phosphorylation measured at 100 μM ATP in the absence and presence (900 μM) of caged ATP using this covalently modified enzyme. The kinetics of phosphorylation is very similar to that shown in Figure 5; the presence of caged ATP induced the formation of a lag phase, while slowing the apparent rate of phosphorylation from 41.5 to 29 s^{-1}. In addition, the steady-state level of ^{32}P incorporation was reduced by 30% compared to that of the unmodified enzyme, implying that a significant fraction of the enzyme had been destroyed. Since about 80% of the Ca-ATPase is labeled by [^{2}H]IASL, we conclude that this inhibition arises predominantly from the treatment with NEM. Moreover, we assume that this inhibition is all-or-none with respect to enzyme activity because the kinetics of the partial reactions

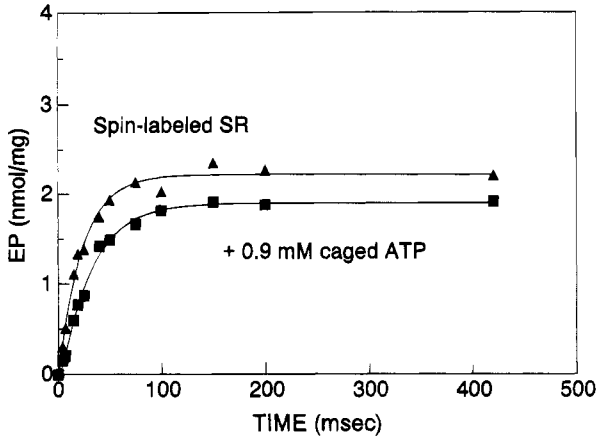

FIGURE 8: Effect of NEM preblock and spin labeling on the pre-steady-state time course of ATP-dependent phosphoenzyme at 2 °C. SR vesicles (0.25 mg/mL) were phosphorylated by 0.1 mM [γ-^{32}P]ATP in standard buffer containing 0.1 M KCl (pH 7.0) either without added caged ATP (▲) or in the presence of 0.9 mM caged ATP (■). The lines represent the best fits to the data using the parameters listed in Table 3.

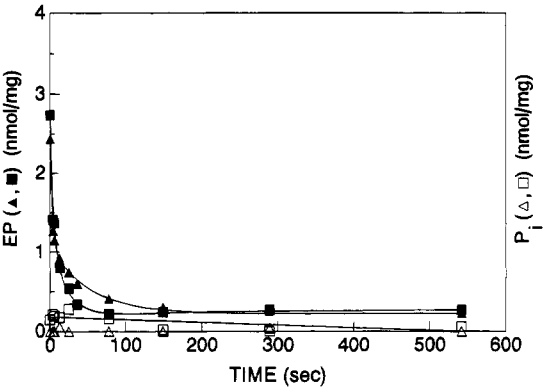

FIGURE 9: Phosphoenzyme decomposition and P_i release at 2 °C following the addition of ADP or ADP + Ca^{2+} (Ca^{2+} jump) to NEM- and [^{2}H]IASL-labeled SR vesicles phosphorylated for 116 ms. The labeled SR vesicles (0.375 mg/mL) were phosphorylated by 0.1 mM [γ-^{32}P]ATP in a solution containing 100 mM KCl (pH 7.0). After 116 ms of phosphoenzyme formation, either (▲, △) 1.66 mM ADP or (■, □) 1.66 mM ADP + 5 mM $CaCl_2$ (final concentrations) was added, and the reaction was terminated at the indicated times by the addition of 3% perchloric acid + 2 mM H_3PO_4. The lines represent the best fits to the data using the parameters listed in Table 4.

in this modified enzyme appear to be normal (see Discussion).

The experiments in Figures 5 and 6 (upper panels) and Table 2 show that the rate constant for the EPR transient is dependent on [KCl]. This provided a useful tool for examining the relationship between the EPR signal and the Ca-ATPase partial reactions, since the latter are also strongly influenced by monovalent salts and ionic strength (Ikemoto, 1981b). The lower panel in Figure 6 shows how raising the [KCl] from 0.1 to 0.4 M affects the time course of phosphorylation in ionophore-treated vesicles. Compared to the results in Figure 5, the most striking change is the biphasic time dependence of phosphorylation, which delayed maximum ^{32}P incorporation by more than 800 ms. By fitting these data to a biexponential function, we obtained rate constants of 57.9 and 2.7 s^{-1} for the fast and slow phases, respectively, with similar levels of ^{32}P incorporation in each phase (Table 3). These rates were essentially unchanged (51.2 and 5.2 s^{-1}) after the enzyme was labeled with NEM and [^{2}H]IASL prior to measuring phosphorylation. In contrast, the presence of caged ATP (900 μM) reduced the fast phase of phosphorylation in the unmodified Ca-ATPase by more than 60% compared to the control, while the slow phase was less strongly inhibited (29%). A comparison of the kinetic data in Table 3 shows that the rate constant for the slow phase of phosphorylation is in approximate agreement with the rate constant for the EPR transient at 0.4 M KCl. This suggests that the EPR signal is tracking a conformational change associated with the slow phase of phosphorylation. In addition, the appearance of the slow phase at high [KCl] implies that [KCl], or possibly ionic strength, has a strong influence on the kinetics of this conformational change.

The presence of biphasic behavior in the phosphorylation reaction at high salt prompted us to reexamine the time course at low (0.1 M) salt using a biexponential curve-fitting function. The results of this analysis, which are summarized in Table 3, show that with one exception (+ caged ATP) fitting the data with two exponentials gave better results than with one. In the absence of caged ATP and covalent modification, the rate constant for the fast phase of EP formation at 0.1 M KCl (48.9 s^{-1}) was in reasonable agreement with that measured at 0.4 M KCl (57.9 s^{-1}), whereas the slow phase was distinctly faster at the lower salt concentration (20.2 vs 2.7 s^{-1}). An additional effect of low [KCl] was a shift in the amount of ^{32}P labeling in the fast and slow phases from 1:1 to 5:1. Treatment with NEM and [^{2}H]IASL did not significantly change these rates, although the disparity between the amplitudes of the two phases was less pronounced (2:1). Comparison of these results to the data in Table 3 shows that the rate constant for the slow phase of phosphorylation, 20.2 s^{-1}, and the rate of the EPR transient measured at low (0.1 M) KCl, 21 s^{-1}, are nearly identical. This parallels the effects seen at high salt and supports a direct correlation between the conformational transition of the EPR transient and the slow phase of phosphorylation.

An exception to the improved results obtained with the biexponential function was the time course of phosphorylation at 0.1 M KCl in the presence of caged ATP. In this case, the monoexponential function proved to be adequate since the two-component equation gave identical parameters for the two phases. This may have resulted from strong inhibition by caged ATP of the initial phase of phosphorylation with a smaller effect on the slow phase, yielding rate constants that differ by less than a factor of 2. Such behavior is, in fact, predicted from the stronger inhibition of the fast phase by caged ATP at 0.4 M KCl.

Dephosphorylation of the Phosphoenzyme by ADP. The reaction mechanism of the Ca-ATPase includes ADP-sensitive (E1P) and ADP-insensitive (E2P) phosphorylated intermediates, which differ with respect to the orientation of their transport sites and Ca^{2+} binding affinities. The proportions of these phosphoenzymes, as well as their kinetic properties, can be evaluated from the pattern of EP decomposition resulting from the addition of ADP at saturating concentrations (Froehlich & Heller, 1985). Figure 9 shows the time course of phosphoenzyme decomposition at 2 °C following the addition of 1.66 mM ADP to NEM- and [^{2}H]-IASL-labeled SR vesicles phosphorylated for 116 ms in a standard buffer containing 100 μM ATP. This initial period

Table 4: ADP Dephosphorylation Fit Parameters[a]

	A_1 (nmol/mg)	k_1 (s^{-1})	A_2 (nmol/mg)	k_2 (s^{-1})
control SR	1.44	>300	1.60	10
+[Ca^{2+}] jump	1.43	>300	1.85	27
spin-labeled SR	1.17	>300	1.05	10
+[Ca^{2+}] jump	1.33	>300	1.22	28

[a] The ADP dephosphorylation data (spin-labeled SR data from Figure 9, control SR data not shown) were fit with the function, $EP(t) = \sum_{n=1}^{3} A_n(e^{-k_n t})$, here A_1 and A_2, and k_1 and k_2 are the amplitudes and decay rates of the ADP-sensitive (E1P) and ADP-insensitive (E2P) phosphoenzymes, respectively, and A_3 and k_3 correspond to a residual phosphoenzyme species (Froehlich & Heller, 1985). In each dephosphorylation experiment, the fast component (k_1) was not resolved, but was estimated by the fits to be greater than 300 s^{-1}. Initial values of A_n and k_n were obtained from semilog plots of the EP decay data, but were allowed to vary freely during the fit. The only constraint imposed was a minimum value of zero for each parameter.

of incubation was sufficient to allow the EP level to reach a steady state (Figure 8). The resulting ADP dephosphorylation pattern was triphasic, consisting of fast (>300 s^{-1}), intermediate (10 s^{-1}), and slow (<1 s^{-1}) components representing 41%, 46%, and 13% of the total phosphoenzyme, respectively (Table 4). Inorganic phosphate production during the dephosphorylation reaction was essentially flat and did not exceed 0.2 nmol of P_i/mg of protein (Figure 9). Addition of 5 mM Ca^{2+} to the ADP chase solution ([Ca^{2+}] jump conditions) increased the decay rate of the intermediate component by 270% without significantly changing the decay fractions (Table 4). The response of the intermediate decay fraction to the increase in [Ca^{2+}] is characteristic of the ADP-insensitive phosphoenzyme, E2P, which contains weak binding sites for Ca^{2+} (Inesi, 1985). At 21 °C, P_i is liberated concurrently with the disappearance of the intermediate component, as predicted for the breakdown of E2P (Froehlich & Heller, 1985). The absence of P_i release during the intermediate decay phase at 2 °C in permeabilized vesicles implies that Ca^{2+} remains associated with E2P subsequent to the isomerization step (possibly as an occluded complex) and is, therefore, able to activate reversal of the phosphoenzyme transition when ADP is added.

A control ADP dephosphorylation experiment using unlabeled SR vesicles gave initial levels of phosphorylation (prior to the chase) that were 30% higher and a decomposition pattern that was quantitatively similar to that obtained with the covalently modified enzyme (Table 4). No P_i production occurred during the dephosphorylation reaction, and 5 mM Ca^{2+} included with ADP in the chase accelerated the decay of the intermediate component, as observed in labeled vesicles (Table 4). These results support the conclusion that labeling with NEM and [^{2}H]IASL reduces the active site concentration, but does not affect the behavior of the remaining sites.

Dephosphorylation of the Phosphoenzyme by EGTA. In order to measure the rate at which E2P is hydrolyzed during ATP-dependent cycling, dephosphorylation experiments were carried out at 2 °C using a chase containing 5 mM EGTA to prevent rephosphorylation of the Ca-ATPase. Mixing was performed by hand because EGTA-induced EP decomposition at 2 °C was too slow to measure in our rapid mixing apparatus. Figure 10 shows an acid quench experiment in which ionophore-treated SR vesicles labeled with NEM and [^{2}H]IASL were phosphorylated with 100 μM ATP for 20 s

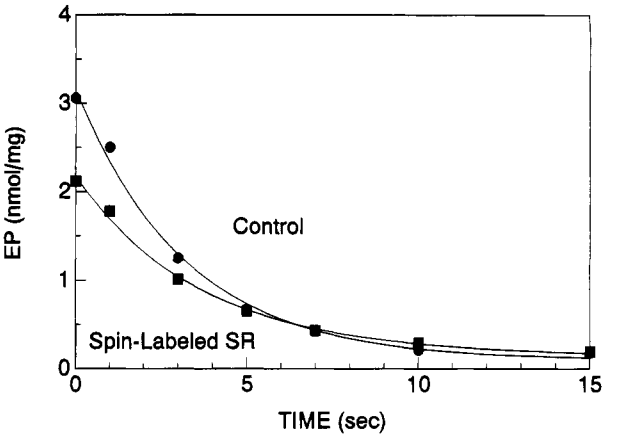

FIGURE 10: Dephosphorylation of the phosphoenzyme by EGTA at 2 °C, measured by hand mixing. Unlabeled (●) or labeled (■) SR vesicles (0.25 mg/mL) were phosphorylated by 100 μM [γ-^{32}P]-ATP in a solution containing 100 mM KCl (pH 7.0) for 20 s, followed by the addition of 5 mM EGTA (final concentration). At the indicated times, the reaction was terminated by the addition of 3% perchloric acid + 2 mM H_3PO_4.

and then chased with 5 mM EGTA (final concentration). The time course of EP decay was monophasic with a rate constant of 0.28 s^{-1}. A small amount (<5%) of residual phosphoenzyme was detected after 10 s that was quite stable to hydrolysis. As in the ADP chase experiments, EGTA-induced dephosphorylation of unlabeled vesicles gave initially higher levels of EP formation and a decay pattern that was similar (k = 0.3 s^{-1}) to that of labeled vesicles. The slow decay of phosphoenzyme induced by EGTA indicates that E2P breakdown in the forward direction at 2 °C is very slow. This effect may reflect a large temperature coefficient for E2P hydrolysis or for Ca^{2+} deocclusion prior to that step.

DISCUSSION

We have used time-resolved EPR and acid quenched-flow experiments in order to study the conformational dynamics of the Ca-ATPase during the pre-steady-state phase of Ca^{2+} pumping. Experiments were carried out at 2 °C to slow the enzyme conformational transients and maximize the effects of substrates on the spectrum. The time course of phosphoenzyme formation at 2 °C is biphasic at both low and high [KCl], and the rate of the transient EPR signal rise directly correlates with the rate of the secondary phosphorylation at both low and high [KCl]. The results provide insight into the transient physical changes in the secondary and tertiary structure of the enzyme associated with the Ca^{2+} translocation process, and they suggest that protein−protein interactions play a role in controlling the conformational changes related to Ca^{2+} translocation.

EPR spectroscopy is uniquely suited for this type of molecular dynamics study. The observed nanosecond spin label motions are much faster than the microsecond motions of the Ca-ATPase as a whole (Squier & Thomas, 1986a,b) and, therefore, must reflect rotational motions within the protein. These could be the motions of a small peptide segment or domain, the Cys side chain to which the spin label is attached, or the spin label itself. These motions are likely to be quite sensitive to local steric factors that change in response to substrate-induced changes in secondary or tertiary structure (i.e., changes in protein conformation), but they are not likely to reflect quaternary structural changes

directly. Since the ATPase undergoes conformational transients during calcium pumping, there will be more than one motional class of labels. Steady-state EPR can be utilized to resolve and quantify the relative contribution of each motional class, which is a key consideration for relating transitions between individual conformational states to the kinetic mechanism. Transient EPR builds on these abilities by adding time resolution, which can be utilized to determine rate constants for transitions between the individual conformational states along the reaction pathway and to detect transient conformational states during enzymatic cycling (Ostap et al., 1993). For example, in the present study we have found that the EPR transient correlates with the slow component of the phosphorylation reaction. Since the chemical kinetic data suggest that this feature represents the activity of a single subunit in an oligomeric complex, our results also suggest that the spin probe is sensing a specific change in Ca-ATPase quaternary structure transmitted through its effect on secondary and tertiary protein structure. Therefore, the combination of biochemical kinetic measurements with steady-state and transient EPR provides a means for unambiguously correlating enzyme structural transitions with specific biochemical intermediates.

Kinetic Resolution of the Conformational Change. The laser flash technique used to trigger the transient change in the fraction of strongly immobilized spin probes contains inherent limitations that may affect the time resolution of these measurements. One of these constraints involves the rate of photolytic conversion of caged ATP to ATP, which is inhibited by Mg^{2+} and alkaline shifts in pH (Barabás & Keszthelyi, 1984; Walker et al., 1988). EPR signals acquired at neutral pH typically displayed an exponential time course preceded by a brief lag phase. We found that lowering the pH from 7 to 6, which increases the rate of photolysis by a factor of 10, abolished the lag in the EPR signal without appreciably changing its rate of formation (Figure 4). For a system of consecutive first-order reactions culminating in the formation of a product, the fastest reactions contribute to the initial lag in product formation, while the slowest reaction in the sequence controls the exponential or burst phase following the lag (Frost & Pearson, 1961). If we visualize photolysis and the spectral changes elicited by ATP release as a two-step process (treating the steps from ATP binding to the conformational transition as one), then it is clear from the results in Figure 4 that ATP release is not rate-limiting for the conformational change at neutral pH. If it had been, then a reduction in the pH would have increased the rate of formation of the signal without affecting the lag. The validity of this conclusion depends on proof that the reactions triggered by ATP release are insensitive to pH over the experimentally tested range. For example, if photolysis were rate-limiting at pH 7 but not at pH 6, then the reactions activated by ATP release (e.g., ATP binding and dissociation, phosphorylation) would have been inhibited by lowering the pH, since they appeared in the lag phase at the prior pH and controlled the burst phase at pH 6. Instead, we found that these reactions were insensitive to this shift in pH (Figure 7), as was the exponential phase of the EPR transient. We conclude that the rate coefficients evaluated from this phase were not distorted by the kinetics of ATP release and that they reflect the true behavior of the underlying reactions. The kinetic delay imposed by the recording system of the EPR spectrometer can also be excluded as a possible source of error because the reciprocal of the time constant (97.7 s^{-1}) is much faster than the transition being measured.

An additional consideration involves the light intensity of the laser flash, which, owing to the turbidity of the SR sample and geometry of the EPR cell, may show a depth-dependent variation parallel to the laser beam. In contrast, we found that a change in the depth of the cell at a constant laser energy did not affect the fraction of ATP released from caged ATP, indicating that the attenuation of light intensity in the beam path was insignificant (see Materials and Methods). This implies that the ATP concentration is uniform throughout the EPR sample cell and that, consequently, the kinetics of the conformational transition is not affected by the geometry of the cell.

Influence of Labeling on Enzyme Kinetics. The specific covalent labeling reagents used in the EPR experiment have the potential for modifying the kinetic behavior of the enzyme and interfering with efforts to identify the signal-producing step. Labeling the enzyme with NEM and [^{2}H]-IASL reduced the level of phosphoenzyme formation by as much as 30%, but did not alter the kinetic behavior of the remaining active sites with respect to ATP-dependent phosphorylation (Table 3). This implies that the labeling procedure did not affect the ATP-induced conformational change (Coan & Keating, 1982) or the formation of (Ca_2)-E1P, but does not exclude possible changes in ATP binding, which require comparative measurements at less than saturating ATP levels. Dephosphorylation by ADP revealed fast, intermediate, and slow decay fractions, whose decomposition rates, [Ca^{2+}] jump sensitivity, and steady-state proportions were unperturbed by labeling with NEM and [^{2}H]-IASL. Moreover, chasing the phosphoenzyme with EGTA, which reveals the spontaneous rate of hydrolysis of E2P, produced behavior that was essentially unaltered by the labeling procedure. These results exclude major effects of the labeling conditions on the principal intermediate reactions of the Ca-ATPase and suggest that any changes resulting from modification by these reagents are all-or-none with respect to their effect on catalytic activity.

Conformational Changes Detected by Time-Resolved EPR. It has previously been demonstrated (Coan & Keating, 1982; Lewis & Thomas, 1992) that the two motional states in the steady-state EPR spectrum of [^{2}H]IASL−Ca-ATPase correspond to two distinct conformational states of the enzyme. Since both states are evident in the presence of a variety of nucleotides, but only one state is evident in the absence of nucleotide, there must be two conformations of the Ca_2·E·nucleotide intermediate. These two conformations have been designated E and E′ for the mobile and restricted populations of probes, respectively (Coan & Keating, 1982), and we use that designation here. Neither enzyme phosphorylation by inorganic phosphate nor stabilization of the enzyme in the E2 conformation induces the E′ component, indicating that the ATPase intermediates producing the strongly immobilized EPR signal, and thus the distinct enzyme conformation, are restricted to Ca_2·E1·MgATP and (Ca_2)E1P states. Since spin label immobilization resulting from the ATP- or AMPPCP-induced conformational transition at the catalytic site is relieved upon the formation of (2Ca)E2P from (Ca_2)E1P, the transient EPR signal reflects net changes in structure coupled to high-energy phosphoenzyme intermediate formation and Ca^{2+} translocation from an external to an internal location.

The effects of substrates and ligands on the IASL−Ca-ATPase spectrum have been extensively characterized by Coan and co-workers (Coan & Inesi, 1977; Coan et al., 1979, 1986; Coan & Keating, 1982; Coan, 1983; Chen et al., 1993), utilizing [^{1}H]-IASL−Ca-ATPase at 25 °C, and by Lewis and Thomas (1992), utilizing [^{2}H]IASL−Ca-ATPase at 4 °C. Comparison of these results with those obtained at 2 °C in the present study shows good agreement, but there is a key difference between our results and those reported by Coan (1983) concerning the effects of enzyme phosphorylation by inorganic phosphate (P_i) in *aqueous* medium on the EPR spectrum. Coan (1983) reports that phosphorylation of the enzyme by P_i broadens the low-field region of the EPR spectrum via the formation of a third motional component having a spectral splitting intermediate between components A and C in our Figure 1 [compare to peaks A and B in Figure 1 of Coan (1983)]. Given the sharper spectral resolution provided by the use of [^{2}H]IASL in these studies (cf. Lewis & Thomas, 1992), we expected to both observe and better resolve this third component, but we could not (Figure 2). It is possible that the low level of E2P that forms from P_i at 2 °C (0.13 nmol/mg) prevented our observation of this component. However, the high-frequency resolution in the [^{2}H]IASL−Ca-ATPase spectrum should have allowed qualitative visualization of this component, even at such low levels (approximately 1 μM EP). We conclude that the conformational state giving rise to the third spectral component in response to phosphorylation by P_i at 25 °C reported by Coan (1983) is either minimized or nonexistent at 2 °C. Nevertheless, even if this component exists and escaped our observation, it is motionally very different from the restricted population of probes that we monitor during the transient EPR experiment, and it does not change the fact that we are selectively monitoring the appearance, steady state, and decay of the restricted population of probes alone.

Coan (1983) also reported a P_i-induced increase in the restricted fraction of the IASL−Ca-ATPase spectrum, but this change could only be observed when 40% dimethyl sulfoxide (DMSO) was added to the phosphorylation medium. Lewis and Thomas (1992) described similar behavior at 4 °C, but they also showed that 40% DMSO alone produces nearly all the changes observed in the DMSO-dependent P_i-phosphorylated [^{2}H]IASL−Ca-ATPase spectrum. Both studies imply that this spectral change is a DMSO effect and not a P_i effect. Therefore, we conclude that the E2P intermediate state has no influence on the restricted component during normal enzyme cycling and that the transient intermediates we observe in the time-resolved EPR experiment are restricted to Ca_2·E1·ATP and (Ca_2)E1P.

Correlation of Enzyme Kinetics with the EPR Transient. As stated earlier, previous studies with [^{2}H]IASL suggest that this probe monitors the formation of the ADP-sensitive phosphoenzyme or an ATP-dependent conformational transition just prior to that step (Coan & Keating, 1982; Lewis & Thomas, 1992). At 2 °C, phosphorylation of the enzyme displayed biphasic kinetics, with a fast phase that was strongly inhibited by caged ATP, but insensitive to KCl, and a slow phase with reversed sensitivity to these ligands. The transient EPR signal showed kinetic behavior resembling that of the slow phase, in that raising the [KCl] from 0.1 to 0.4 M decreased its rate of formation. In addition, the rate constants for the EPR transient and the slow phase of phosphorylation were nearly identical at both low (20 s^{-1}) and high (4−6 s^{-1}) [KCl]. This comparison does not take into account an additional inhibitory effect of caged ATP, which at high [KCl] reduced the rate of the slow phase by about 29% relative to that of the control. At 0.1 M KCl, we were able to resolve only a single phase of phosphorylation with an apparent rate of 27 s^{-1} because of strong inhibition of the fast phase by caged ATP. From the rate of the slow phase in the absence of caged ATP (20 s^{-1}), and the inhibition produced by caged ATP at high [KCl], we estimate that the slow phase has a rate of about 15 s^{-1} at 0.1 M KCl, which is similar to the rate of the EPR transient at low salt (20 s^{-1}). At 0.4 M KCl, the rate of the EPR transient had a rate of 5.3 s^{-1} and, thus, behaved more like the slow phase in the presence of caged ATP (1.9 s^{-1}) than the fast phase (21 s^{-1}). We conclude from these results that the EPR transient tracks events linked to the formation of the slow component of phosphorylation.

Scheme 3

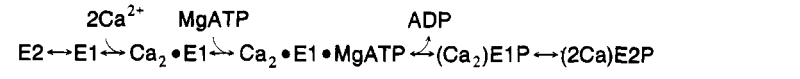

EPR experiments in this study, and those previously reported by Coan and Keating (1982) utilizing nonhydrolyzable ATP analogs, indicate that phosphorylation is preceded by an ATP-induced conformational change, which is rate-limiting for ^{32}P incorporation at 21 °C (Petithory & Jencks, 1986). We assume that phosphoenzyme formation in the slow phase at 2 °C is preceded by a similar conformational event and that the EPR transient most likely coincides with the formation of Ca_2·E1′·MgATP, where the prime designates the ATP-induced conformational state. Since phosphoenzyme formation follows this step, it will be delayed with respect to the EPR signal and will produce rates that are slower. This may, in fact, account for the less than perfect agreement between the rate constants evaluated from the quenched-flow and EPR experiments. It is interesting to note that the kinetics of the fast phase of phosphorylation was not affected by increasing the KCl concentration from 0.1 to 0.4 M (Table 3). This suggests that the rate of the ATP-induced conformational change in the slow phase is itself controlled by another step that is quite sensitive to [KCl] or a change in ionic strength.

Ca-ATPase Oligomer Model. Biphasic phosphorylation kinetics has been observed in both the Ca- and Na,K-ATPases under a variety of conditions (Hobbs et al., 1985). Ikemoto et al. (1981b) demonstrated that high levels of choline chloride were able to induce biphasic behavior, which was presented as evidence for an oligomeric Ca^{2+} pump. In the present study, exposure to high [KCl] produced a biphasic phosphorylation pattern with a 50:50 distribution of fast and slow phases. Before we present a model to account for this biphasic behavior, it is important to consider why simple consecutive transport schemes are excluded from this behavior. In principle, this pattern could arise from an equilibrium mixture of the E1 and E2 conformers (see Scheme 3), which undergo slow interconversion. The conformational change triggered by ATP and the reactions occurring subsequent to the phosphoenzyme transition have been left out of Scheme 3 for simplicity. Addition of MgATP and Ca^{2+} to an equilibrium mixture of E1 and E2 will produce a rapid initial phase of phosphorylation corresponding to ^{32}P labeling of enzyme in the E1

Scheme 4

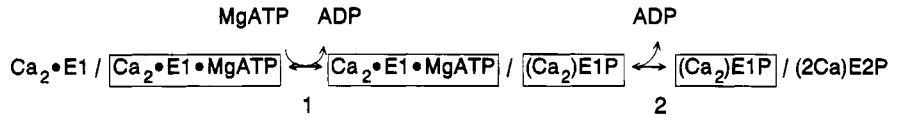

conformation and will be followed by a slower phase reflecting the conversion of E2 to E1. If such a mixture of these states occurs, it can only happen in the absence of Ca^{2+}, which will stabilize E2. The 3.5 μM Ca^{2+} employed in our experiments should have been sufficient to convert all of the enzyme to the high-affinity E1 state (Alonso & Hecht, 1990). Biphasic kinetics can also arise from a rapidly reversible phosphorylation reaction followed by a slow, irreversible phosphoenzyme isomerization step (Hobbs et al, 1988). In this case, the fast phase corresponds to the formation of (Ca_2)E1P, which is in rapid equilibrium with Ca_2•E1•MgATP. Subsequent conversion to the ADP-insensitive phosphoenzyme shifts this quasi-equilibrium to the right, causing further depletion of the enzyme−substrate complex and a slow rise in the phosphoenzyme level. In order to have significant reversal of the phosphorylation reaction, ADP accumulation during the pre-steady state must be significant relative to the $K_{0.5}$ for the back-reaction, which is about 100 μM (Pickart & Jencks, 1982; Wang, 1986). Because the active site density in our experiments was less than 1 μM, this condition was never achieved. Moreover, we have evidence at 2 °C (Froehlich et al., unpublished) that conversion of the ADP-sensitive to the ADP-insensitive phosphoenzyme occurs rapidly during the initial cycle of ATP hydrolysis, eliminating the second requirement. We conclude that the conditions required to elicit biphasic phosphorylation from Scheme 3 do not occur in our rapid mixing experiments and that other factors are responsible for this complex behavior.

Parallel pathways of ATP hydrolysis involving independent enzyme populations with different catalytic activities may also produce biphasic phosphorylation kinetics. Isoforms constitute a likely source for this behavior, although fast-twitch skeletal muscle contains only a single Ca-ATPase isoform (MacLennan et al., 1992). If parallel catalytic pathways are responsible for the biphasic pattern, then the enzyme populations must be present in equal amounts to satisfy the 50:50 distribution of fast and slow components reported here. A more stringent set of constraints derives from experiments with $C_{12}E_8$, which can induce the formation of monomers (Dean & Tanford, 1978). Ikemoto et al. (1981a) found that solubilization with $C_{12}E_8$ transformed the enzyme to a single catalytic species, while removal of the detergent restored kinetic heterogeneity. These kinetic properties do not exclude the participation of parallel pathways, but are sufficiently unique to render this explanation unlikely.

The central feature that distinguishes these independent pathway models from oligomeric schemes is the evidence for communication between the transport units during catalysis. Oligomeric models for the Ca-ATPase (Froehlich & Taylor, 1976; Ikemoto et al., 1981a,b; Froehlich & Heller, 1985) postulate coupling of the catalytic activity of the subunits, which constrains them to an alternating or staggered mode of operation. This order is imposed by a conformational interaction between the subunits in accordance with the quaternary structure of the system. The [^{2}H]IASL spin probe is expected to monitor the conformational events in the entire enzyme population, but it only reports on the slow phase of phosphorylation. This behavior can be explained by an oligomer hypothesis in which the operation of the subunits and the rapid conversion of E1P to E2P prevent the detection of spin probes monitoring the rapid phase of phosphorylation. This model is illustrated in Scheme 4, in which the boxes indicate the intermediates detected by EPR as the restricted components. We assume that the subunit undergoing phosphorylation initially is rapidly transformed to an ADP-insensitive state, which does not produce a signal. The lifetime of (Ca_2)E1P on the right-hand subunit is so short that the signal associated with that state is not resolved. Ca_2•E1•MgATP may also contribute to the fraction of strongly immobilized spin labels, but it too has a very transient existence. In contrast, the ADP-sensitive phosphoenzyme on the left-hand subunit (Scheme 4) has a much longer lifetime by virtue of tight conformational coupling to (2Ca)-E2P, which very slowly releases Ca^{2+} to the SR lumen (Beeler & Keffer, 1984). These features are consistent with the roughly equal amounts of ADP-sensitive and ADP-insensitive phosphoenzymes in the steady state (Figure 9 and Table 4), the slow turnover of E2P to P_i (Figure 10), and the slow release of Ca^{2+} to the inside of the vesicle at 2 °C (Beeler & Keffer, 1984). The prediction that half of the subunits undergo rapid transformation to an E2P state during cycling would also explain why the amplitude of the EPR signal produced by the nonhydrolyzable ATP analog is approximately twice that found with ATP (Table 1). This assumes that both subunits can be occupied by these analogs and can produce stable EPR signals when turnover is prevented. An essential requirement of the oligomer hypothesis is that the transformation of E1P to E2P be much faster than ^{32}P incorporation during the rapid phase of phosphorylation at 2 °C (about 50 s^{-1}). Preliminary results from dephosphorylation experiments with ADP support this prediction.

Although the high KCl levels used in this study enhanced resolution of the biphasic phosphorylation kinetics, they were not essential for the demonstration of this pattern or the monophasic EPR signal. This supports the view that this behavior has relevance to Ca^{2+} transport at physiological ionic strength. Although the biphasic pattern seen at 2 °C is not resolved at higher temperatures except in special circumstances (Hobbs et al., 1985), certain features of the complex kinetic behavior are retained at 21 °C and implicate the presence of subunit−subunit interactions (Froehlich & Heller, 1985). Strong quaternary interactions may occur at several points in the transport cycle, possibly serving as a means of energy conservation. We propose that the formation of weakly associated oligomeric complexes may be necessary in between these steps to allow progression to a subsequent conformational state. Indeed, previous studies in our laboratory (see below) have shown that dynamic changes in the oligomeric state of the Ca-ATPase do correlate with optimum enzymatic activity. The secondary phase of phosphorylation detected by the [^{2}H]IASL probe may, in fact,

be rate-limited by a slow quaternary change, producing a loosely associated complex in response to ATP binding. High [KCl] or salts such as choline chloride (Ikemoto et al., 1981b) may act to slow this transition and the subsequent phosphorylation by promoting aggregation of the subunits. That high [KCl] does not delay the slow phase by preventing ATP binding or directly interfering with phosphorylation is suggested by the fact that the fast phase of phosphoenzyme formation was not inhibited by an elevation in [KCl] (Table 3). At 0.1 M KCl, the fast phase exceeded the slow phase in amplitude, which could mean that the association between subunits is weakened by these conditions. Whether this signifies the accumulation of a functionally monomeric enzyme in parallel with the oligomer or the presence of a more transient interaction between subunits is a question that cannot be resolved by these measurements.

Relationship to Previous Studies. A number of physical studies have provided evidence that Ca-ATPase protein−protein interactions may play a functional role in the kinetic cycle of the enzyme, including electron microscopy studies [reviewed by Martonosi et al., (1990); Scales & Inesi, 1976; Napolitano et al. (1983)] and fluorescence energy transfer (Vanderkooi et al., 1977; Bigelow et al., 1992). In our laboratory, we have used saturation-transfer EPR (Squier & Thomas, 1988; Squier et al., 1988; Lewis & Thomas, 1986) and time-resolved phosphorescence anisotropy [Birmachu & Thomas, 1990; reviewed by Thomas and Mahaney (1993)] to study the relationship between the oligomeric state of the Ca-ATPase and Ca^{2+}-transport activity. There is now a large body of work indicating that the Ca-ATPase can be inhibited in the SR membrane by perturbations that overstabilize either large oligomers [Birmachu & Thomas, 1990; Mahaney & Thomas, 1991; reviewed by Thomas and Karon (1994)] or monomers (Karon & Thomas, 1993; Kutchai et al., 1993) of the enzyme. These results indicate that the Ca-ATPase primarily exists as small oligomers (dimer, tetramer) under physiological conditions and that it has optimal activity in these small oligomers, consistent with the results of the present study.

Conclusions. The present study demonstrates that transient EPR offers the opportunity to detect and resolve conformational transients in the Ca-ATPase during the pre-steady-state phase of calcium translocation. By pairing our EPR studies with quenched-flow experiments, we have directly correlated the dynamic physical states of the protein with biochemical kinetics of Ca^{2+} transport, and our results support the conclusion that subunit−subunit interactions play a role in controlling conformational changes related to Ca^{2+} translocation. Continued integration of physical and biochemical kinetic studies should prove to be a valuable means for obtaining important insight into the relationships between the molecular dynamics of the Ca-ATPase, the enzyme's oligomeric state, and specific steps in its catalytic mechanism. For example, this approach should provide important insight into the effects of the regulatory peptide phospholamban on the molecular dynamics and kinetics of the Ca-ATPase of the cardiac SR membrane.

ACKNOWLEDGMENT

We are grateful to Dr. Al Beth (Vanderbilt University) for providing [^{2}H]IASL and to Cindy Klevikis and Charles Grisham (University of Virginia) for providing the CrATP. We thank Phuong Nguyen, Erin Nissen, and Phil Heller for technical assistance, Mike Ostap for advice on optimizing the transient EPR experiments, Bob Bennett for developing our EPR analysis software, maintaining our spectrometer and laser, and handling instrument troubleshooting and repair, and Franz Nisswandt and Nicoleta Cornea for help with our computer network and file server.

REFERENCES

Alonso, G. L., & Hecht, J. P. (1990) *J. Theor. Biol. 147*, 161−176.
Arrondo, J. L. R., Mantsch, H. H., Mullner, N., Pikula, S., & Martonosi, A. (1987) *J. Biol. Chem. 262*, 9037−9043.
Barabás, K., & Keszthelyi, L. (1984) *Acta Biochim. Biophys. Acad. Sci. Hung. 19*, 305−309.
Barth, A., Kreutz, W., & Mäntele, W. (1990) *FEBS Lett. 277*, 147−150.
Barth, A., Mäntele, W., & Kreutz, W. (1991) *Biochim. Biophys. Acta 1057*, 115−123.
Beeler, T., & Keffer, J. (1984) *Biochim. Biophys. Acta 773*, 99−105.
Berger, C. L., & Thomas, D. D. (1991) *Biochemistry 30*, 11036−11045.
Berger, C. L., Svensson, E. C., & Thomas, D. D. (1989) *Proc. Natl. Acad. Sci. U.S.A. 86*, 8753−8757.
Bigelow, D. J., Squier, T. C., & Thomas, D. D. (1986) *Biochemistry 25*, 194−202.
Bigelow, D. J., Squier, T. C., & Inesi, G. (1992) *J. Biol. Chem. 267*, 6952−6962.
Birmachu, W., & Thomas, D. D. (1990) *Biochemistry 29*, 3904−3914.
Birmachu, W., Nisswandt, F. L., & Thomas, D. D. (1989) *Biochemistry 28*, 3940−3947.
Blasie, J. K., Pascolini, D., Asturias, F., Herbette, L. G., Pierce, D., & Scarpa, A. (1990) *Biophys. J. 58*, 687−693.
Buchet, R., Jona, I., & Martonosi, A. (1992) *Biochim. Biophys. Acta 1104*, 207−214.
Champeil, P., Le Maire, M., Moller, J. V., Riollet, S., Guillain, F., & Green, N. M. (1986) *FEBS Lett. 206*, 93−98.
Chen, P. S., Toribara, T. Y., & Warner, H. (1956) *Anal. Chem. 28*, 1756−1758.
Chen, Z., Coan, C., Fielding, L., & Cassafer, G. (1991) *J. Biol. Chem. 266*, 12386−12394.
Coan, C. (1983) *Biochemistry 22*, 5826−5836.
Coan, C., & Inesi, G. (1977) *J. Biol. Chem. 252*, 3044−3049.
Coan, C., & Keating, S. (1982) *Biochemistry 21*, 3214−3220.
Coan, C., Verjovski-Almeida, S., & Inesi, G. (1979) *J. Biol. Chem. 254*, 2968−2974.
Coan, C., Scales, D. J., & Murphy, A. J. (1986) *J. Biol. Chem. 261*, 10394−10403.
Dean, W. L., & Tanford, C. (1978) *Biochemistry 17*, 1683−1690.
Dupont, Y. (1976) *Biochem. Biophys. Res. Commun. 71*, 544−550.
Dupont, Y. (1980) *Eur. J. Biochem. 109*, 231−238.
Fajer, P. G., Fajer, E. A., & Thomas, D. D. (1990) *Proc. Natl. Acad. Sci. U.S.A. 87*, 5538−5542.
Fernandez, J. L., Rosemblatt, M., & Hidalgo, C. (1980) *Biochim. Biophys. Acta 599*, 552−568.
Freed, J. (1976) in *Spin Labeling-Theory and Applications* (Berliner, L. J., Ed.) pp 567−571, Academic Press, New York.
Froehlich, J. P., & Taylor, E. W. (1975) *J. Biol. Chem. 250*, 2013−2021.
Froehlich, J. P., & Taylor, E. W. (1976) *J. Biol. Chem. 251*, 2307−2315.
Froehlich, J. P., & Heller, P. F. (1985) *Biochemistry 24*, 126−136.
Froehlich, J. P., Sullivan, J. V., and Berger, R. L. (1976) *Anal. Biochem. 73*, 331−341.
Frost, A. A., & Pearson, R. G. (1961) in *Kinetics and Mechanism,* 2nd ed., pp 166−169, John Wiley & Sons, Inc., New York.
Froud, R. J., & Lee, A. G. (1986) *Biochem. J. 237*, 197−206.
Gornall, A. G., Bardawill, C. J., & David, M. M. (1949) *J. Biol. Chem. 177*, 751−766.

Hanel, A. M., & Jencks, W. P. (1991) *Biochemistry 30*, 11320−11330.
Hobbs, A. S., Albers, R. W., Froehlich, J. P., & Heller, P. F. (1985) *J. Biol. Chem. 260*, 2035−2037.
Hobbs, A. S., Albers, R. W., & Froehlich, J. P. (1988) in *The Na^+,K^+-Pump, Part A* (Skou, J. C., Nørby, J. G., Maunsbach, A. B., & Esmann, M., Eds.) pp 307−314, Ellen R. Liss, Inc., New York.
Ikemoto, N., Garcia, A. M., Kurobe, Y., & Scott, T. L. (1981a) *J. Biol. Chem. 256*, 8593−8601.
Ikemoto, M., Miyao, A., & Kurobe, Y. (1981b) *J. Biol. Chem. 256*, 10809−10814.
Inesi, G. (1985) *Annu. Rev. Physiol. 47*, 573−601.
Inesi, G., Sumbilla, C., & Kirtley, M. E. (1990) *Physiol. Rev. 70*, 749−760.
Inesi, G., Cantilia, T., Yu, X., Nikic, D., Sagara, Y., & Kirtley, M. E. (1992) *Ann. N.Y. Acad. Sci. 671*, 32−48.
Kanazawa, T., & Boyer, P. D. (1973) *J. Biol. Chem. 248*, 3163−3172.
Karon, B. S., & Thomas, D. D. (1993) *Biochemistry 32*, 7503−7511.
Karon, B. S., Mahaney, J. E., & Thomas, D. D. (1994) *Biochemistry* (in press).
Knott, G. D. (1979) *Comput. Programs Biomed. 10*, 271−280.
Kubo, K., Suzuki, H., & Kanazawa, T. (1990) *Biochim. Biophys. Acta 1040*, 251−259.
Kutchai, H., Mahaney, J. E., Geddis, L. M., & Thomas, D. D. (1993) *Biophys. J. 64*, A306.
Lacapere, J.-J., & Guillain, F. (1993) *Eur. J. Biochem. 211*, 117−126.
Lanzetta, P. A., Alvarez, L. J., Reinach, P. S., & Candia, D. A. (1979) *Anal. Biochem. 100*, 95−97.
Lewis, S. M., & Thomas, D. D. (1986) *Biochemistry 25*, 4615−4621..
Lewis, S. M., & Thomas, D. D. (1991) *Biochemistry 30*, 8331−8139.
Lewis, S. M., & Thomas, D. D. (1992) *Biochemistry 31*, 7381−7389.
MacLennan, D. H. (1990) *Biophys. J. 58*, 1355−1365.
MacLennan, D. H., & Toyofuku, T. (1992) *Annals NY Acad. Sci. 671*:1−10.
Martonosi, A. N., Jona, I., Molnar, E., Seidler, N., Buchet, R., & Varga, S. (1990) *FEBS Lett. 268*, 365−370.
McCray, J. A., & Trentham, D. R. (1989) *Annu. Rev. Biophys. Biophys. Chem. 18*, 239−270.
Murphy, A. (1978) *J. Biol. Chem. 253*, 385−389.
Napolitano, C. A., Cooke, P., Segalman, K., & Herbette, L. (1983) *Biophys. J. 42*, 119−125.
Obara, M., Suzuki, H., & Kanazawa, T. (1988) *J. Biol. Chem. 263*, 3690−3697.
Orlowski, S., & Champeil, P. (1991) *Biochemistry 30*, 11331−11342.
Ostap, E. M., & Thomas, D. D. (1991) *Biophys. J. 59*, 1235−1241.
Ostap, E. M., White, H. D., & Thomas, D. D. (1993) *Biochemistry 32*, 6712−6720.
Petithory, J. R., & Jencks, W. P. (1986) *Biochemistry 25*, 4493−4497.
Pick, V., & Bassilian, S. (1981) *FEBS Lett. 123*, 127−136.
Pickart, C. M., & Jencks, W. P. (1982) *J. Biol. Chem. 257*, 5319−5322.
Pierce, D. H., Scarpa, A., Topp, M. R., & Blasie, J. K. (1983) *Biochemistry 22*, 5254−5261.
Ross, D. C., Davidson, G. A., & McIntosh, D. B. (1991) *J. Biol. Chem. 266*, 4613−4621.
Scales, D. J., & Inesi, G. (1976) *Arch. Biochem. Biophys. 176*, 392−394.
Shigekawa, M., & Dougherty, J. P. (1978) *J. Biol. Chem. 253*, 1458−1464.
Shigekawa, S., & Kanazawa, T. (1982) *J. Biol. Chem. 257*, 7657−7665.
Shigekawa, M., Dougherty, J. P., & Katz, A. M. (1978) *J. Biol. Chem. 253*, 1442−1450.
Squier, T. C., & Thomas, D. D. (1986a) *Biophys. J. 49*, 921−935.
Squier, T. C., & Thomas, D. D. (1986b) *Biophys. J. 49*, 937−942.
Squier, T. C., & Thomas, D. D. (1988) *J. Biol. Chem. 263*, 9171−9177.
Squier, T. C., & Thomas, D. D. (1989) *Biophys. J. 56*, 735−748.
Squier, T. C., Hughes, S. E., & Thomas, D. D. (1988) *J. Biol. Chem. 263*, 9162−9170.
Sumida, M., Wang, T., Schwartz, A., Younkin, C., & Froehlich, J. P. (1980) *J. Biol. Chem. 255*, 1497−1503.
Suzuki, H., Obara, M., Kuwayama, H., & Kanazawa, T. (1987) *J. Biol. Chem. 262*, 15448−15456.
Suzuki, H., Obara, M., & Kanazawa, T. (1989) *J. Biol. Chem. 264*, 920−927.
Thomas, D. D., & Mahaney, J. E. (1993) *New Comp. Biochem. 25*, 301−319.
Thomas, D. D., & Karon, B. S. (1994) in *The Temperature Adaptation of Biological Membranes* (Cossins, A., Ed.) Portland Press, London (in press).
Thomas, D. D., Ostap, E. M., Berger, C. L., Lewis, S. M., Fajer, P. G., & Mahaney, J. E. (1993) *Biol. Magn. Reson. 13*, 323−351.
Toyoshima, C., Sasabe, H., & Stokes, D. L. (1993) *Nature 362*, 469−471.
Vanderkooi, J. M., Ierokomas, A., Nakamura, H., & Martinosi, A. (1977) *Biochemistry 16*, 1262−1267.
Vilsen, B., & Andersen, J. P. (1987) *Biochim. Biophys. Acta 898*, 313−322.
Wakabayashi, S., Ogurusu, T., & Shigekawa, M. (1986) *J. Biol. Chem. 261*, 9762−9769.
Wakabayashi, S., Imagawa, T., & Shigekawa, M. (1990a) *J. Biochem. 107*, 563−571.
Wakabayashi, S., Ogurusu, T., & Shigekawa, M. (1990b) *Biochemistry 29*, 10613−10620.
Walker, J. W., Reid, G. P., McCray, J. A., & Trentham, D. R. (1988) *J. Am. Chem. Soc. 110*, 7170−7177.
Wang, T. (1986) *J. Biol. Chem. 261*, 6307−6316.
Wawrzynow, A., Collins, J. H., & Coan, C. (1993) *Biochemistry 32*, 10803−10811.
Yamada, S., & Ikemoto, N. (1978) *J. Biol. Chem. 253*, 6801−6807.
Zang, Z., Sumbilla, C., Lewis, D., & Inesi, G. (1993) *FEBS Lett. 335*, 261−264.

BI942458H